Electronic Supplementary Information for:

N-Heterocyclic Silylene Complexes of Group VI Transition Metal Carbonyls

Eduard Glok[a], Moritz Schanbacher[a], Christian Luz[a] and Udo Radius[a]*.

[a]*Institut für Anorganische Chemie, Julius-Maximilians-Universität Würzburg, Am Hubland, 97074 Würzburg, Germany.*

Content:

1) Additional Figures

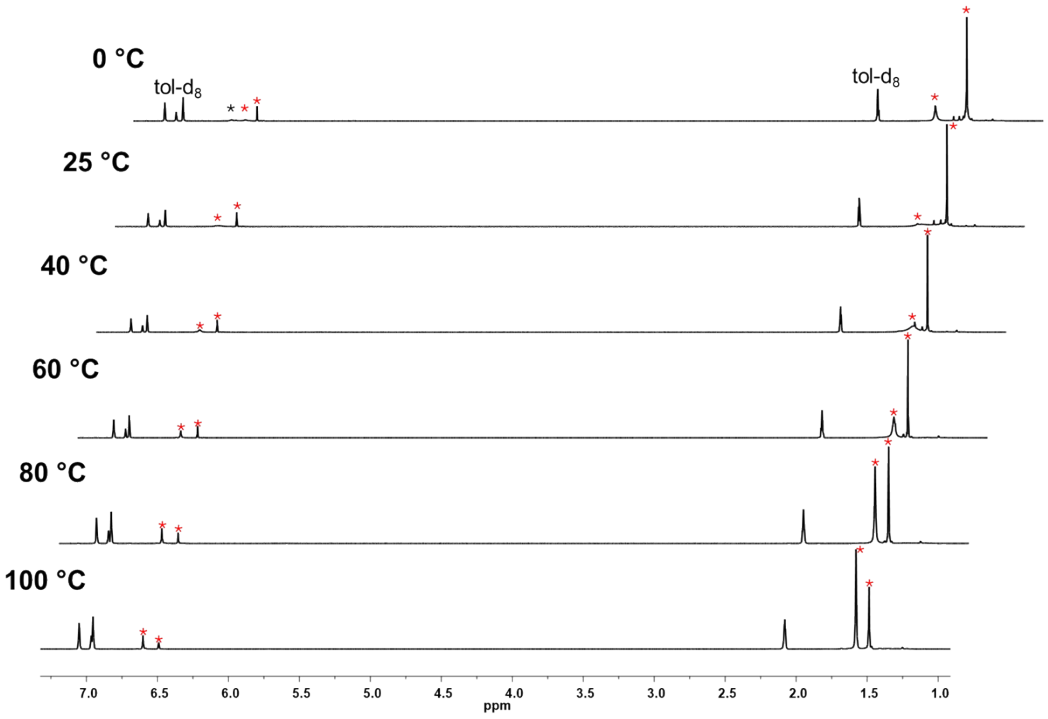

Figure S1. ^{1}H NMR spectra (600.2 MHz, toluene-d_8, 298–373 K) of [Mo(*t*Bu$_2$NHSi)$_3$(CO)$_3$] **2**, part 1. Signals marked with an asterisk belong to the silylene ligands.

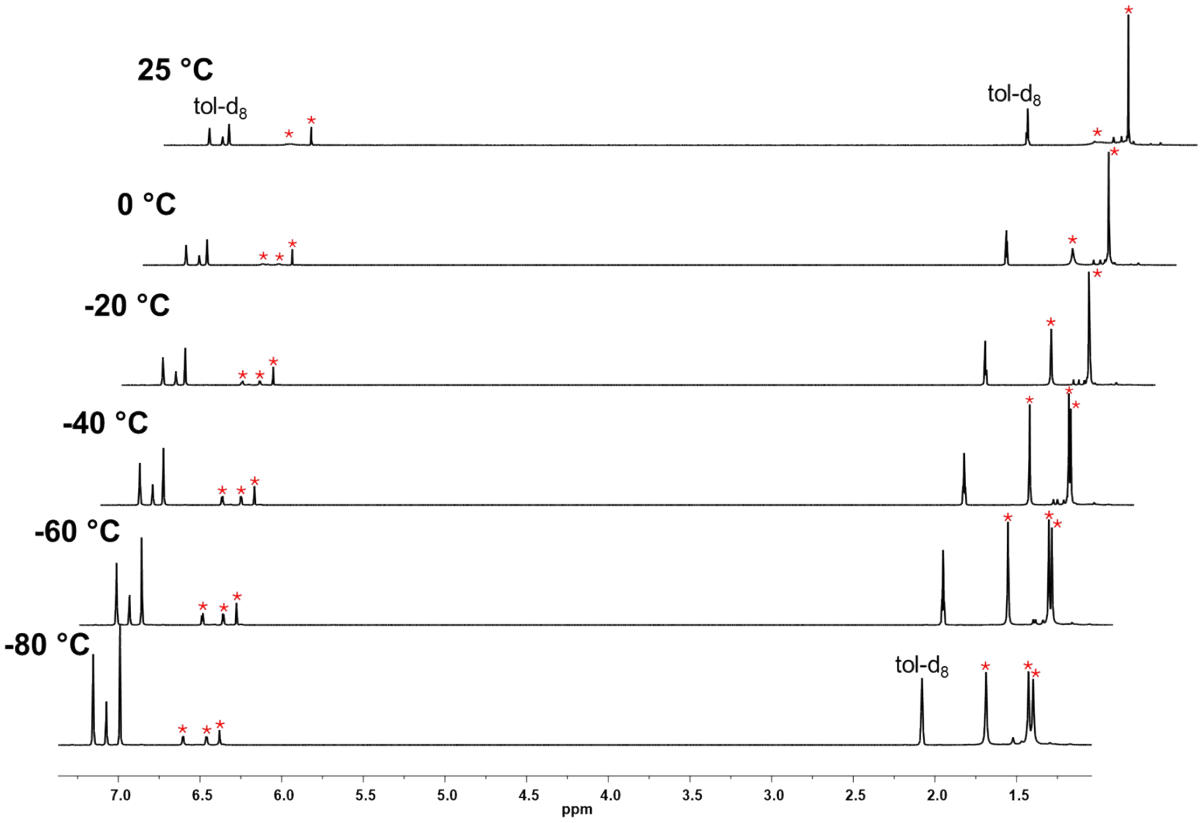

Figure S2. ^{1}H NMR spectrum (600.2 MHz, toluene-d_8, 193–298 K) of [Mo(tBu$_2$NHSi)$_3$(CO)$_3$] **2**, part 2. Signals marked with an asterisk belong to the silylene ligands.

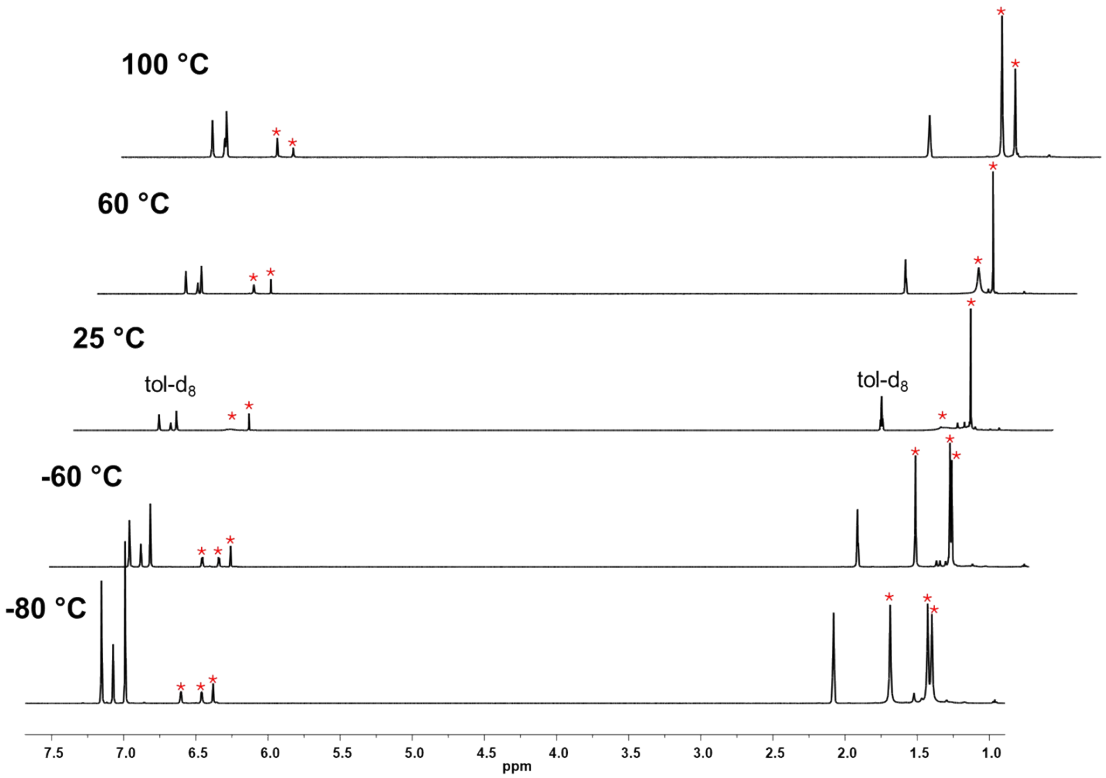

Figure S3. ^{1}H NMR spectra (600.2 MHz, toluene-d_8, 193–373 K) of [Mo(tBu$_2$NHSi)$_3$(CO)$_3$] **2**, part 3. Signals marked with an asterisk belong to the silylene ligands.

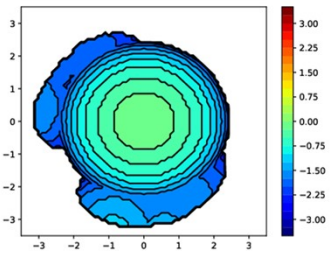

cis-Mes$_2$NHSi:
%V_{bur} (d = 2.5 Å; r = 3.5 Å) = 24.6

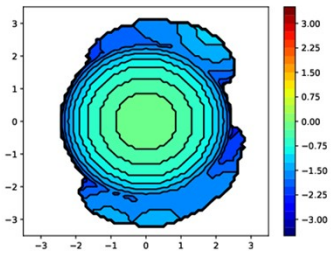

trans-Mes$_2$NHSi:
%V_{bur} (d = 2.5 Å; r = 3.5 Å) = 25.1

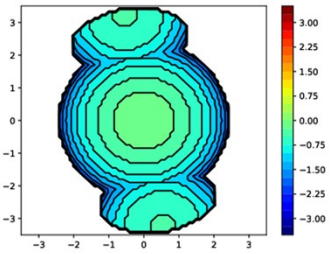

cis-tBu$_2$NHSi:
%V_{bur} (d = 2.5 Å; r = 3.5 Å) = 27.6

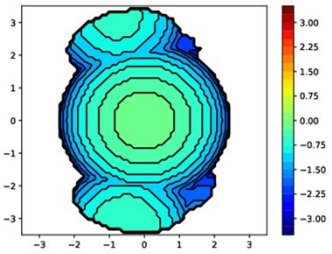

trans-tBu$_2$NHSi:
%V_{bur} (d = 2.5 Å; r = 3.5 Å) = 27.1

Figure S4. Steric maps and calculated $\%V_{bur}$ (percent buried volume) of the *cis*- and *trans*-positioned N-heterocyclic silylenes tBu$_2$NHSi and Mes$_2$NHSi in the molybdenum complexes [Mo(R$_2$NHSi)$_3$(CO)$_3$] **2** and **3**.

2) NMR and IR spectra of the compounds 1-9

[Cr(*t*Bu$_2$NHSi)$_3$(CO)$_3$] (1)

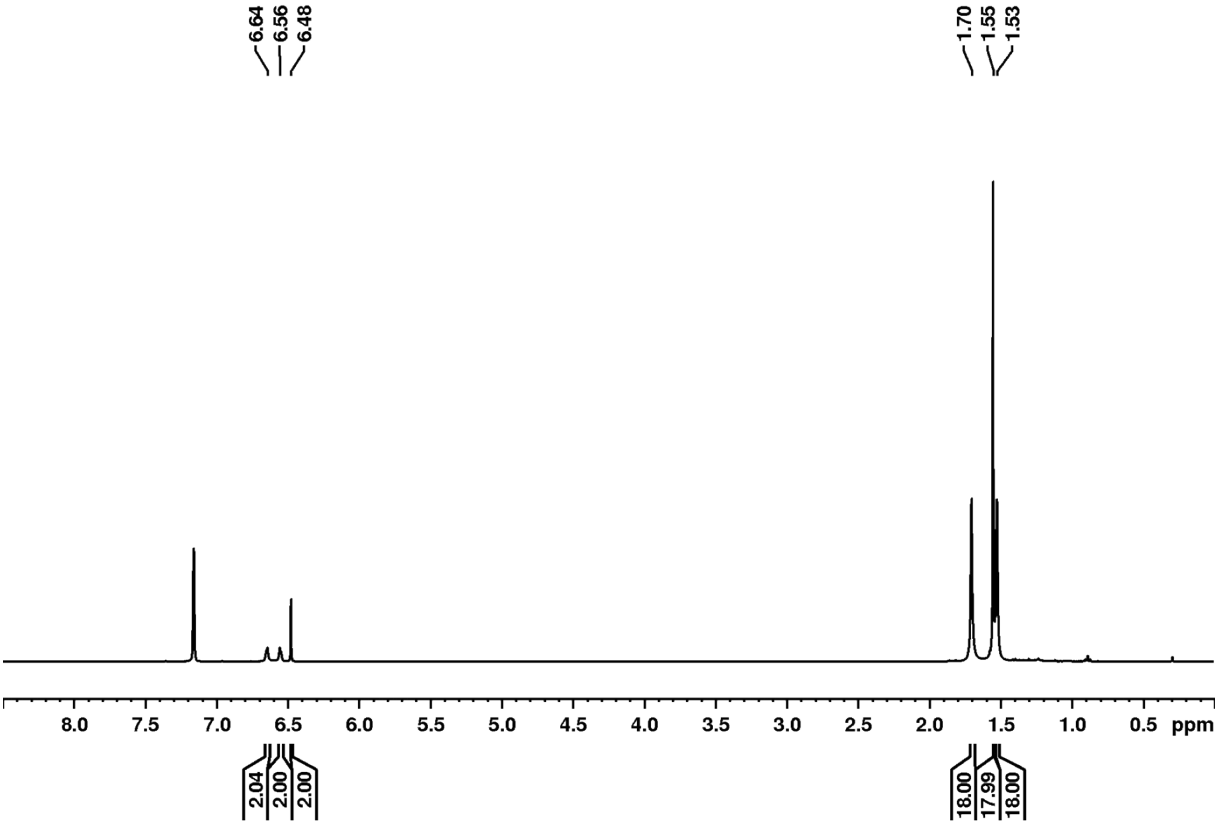

Figure S5. ^{1}H NMR spectrum (400.1 MHz, C_6D_6, 298 K) of [Cr(*t*Bu$_2$NHSi)$_3$(CO)$_3$] (**1**).

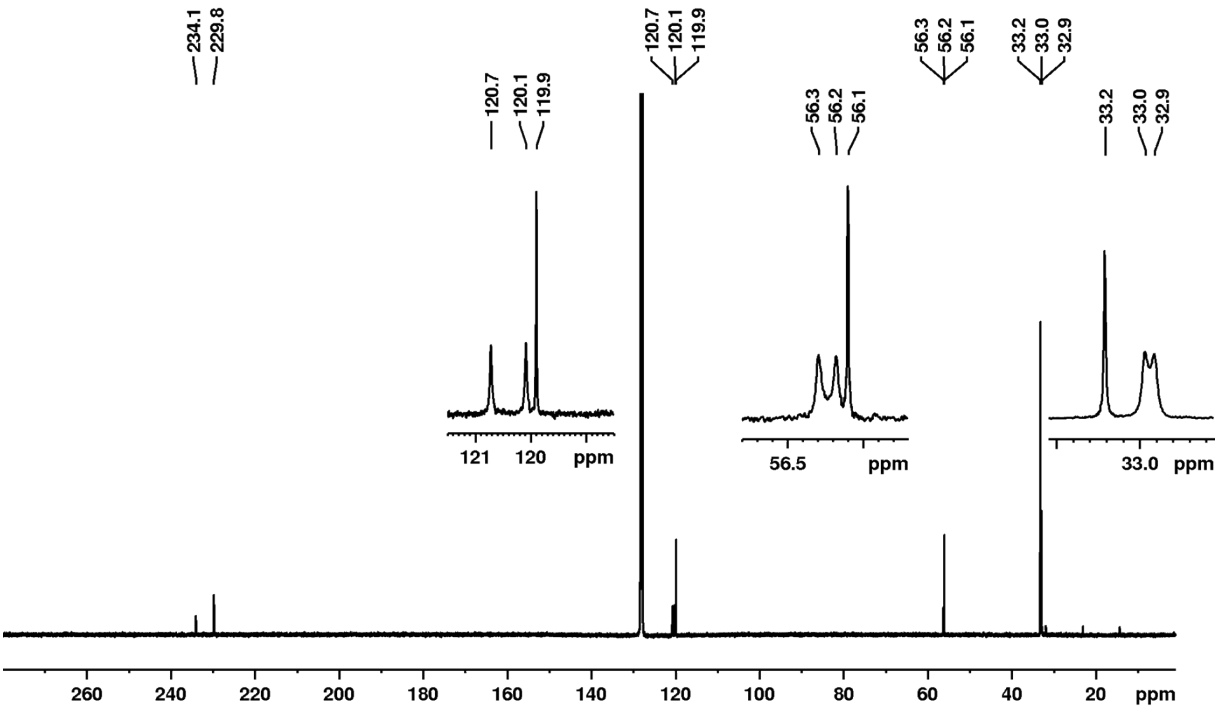

Figure S6. ^{13}C{^{1}H} NMR spectrum (100.6 MHz, C_6D_6, 298 K) of [Cr(*t*Bu$_2$NHSi)$_3$(CO)$_3$] (**1**).

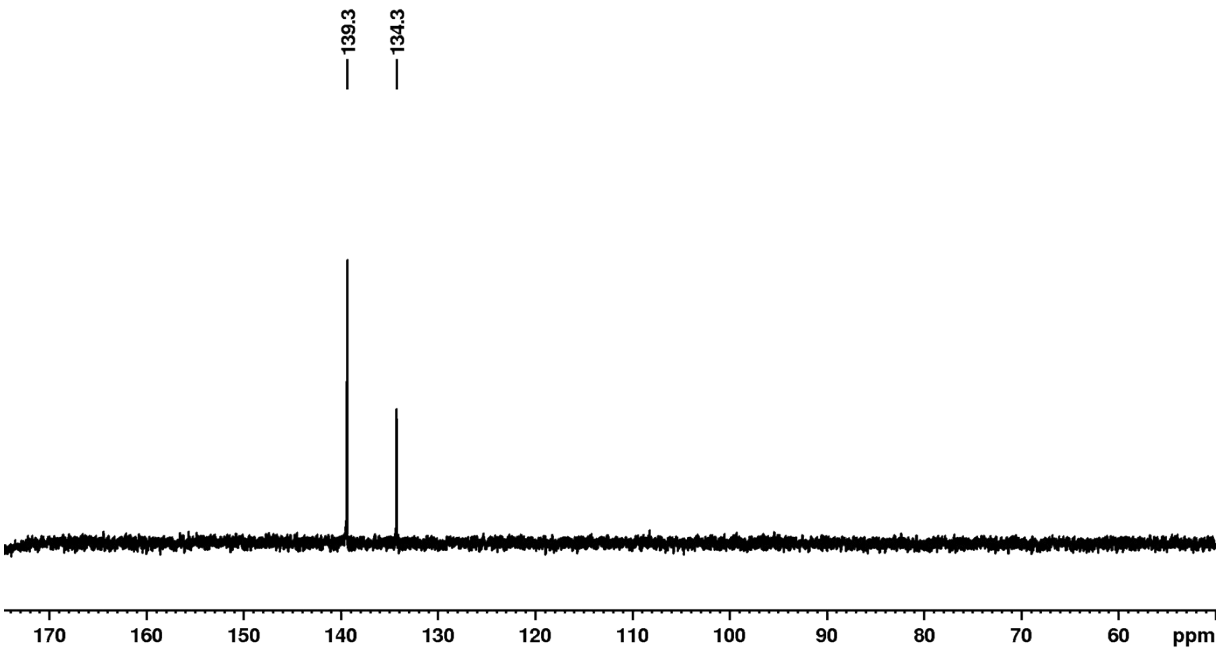

Figure S7. $^{29}Si\{^{1}H\}$ NMR spectrum (79.5 MHz, C_6D_6, 298 K) of $[Cr(tBu_2NHSi)_3(CO)_3]$ (**1**).

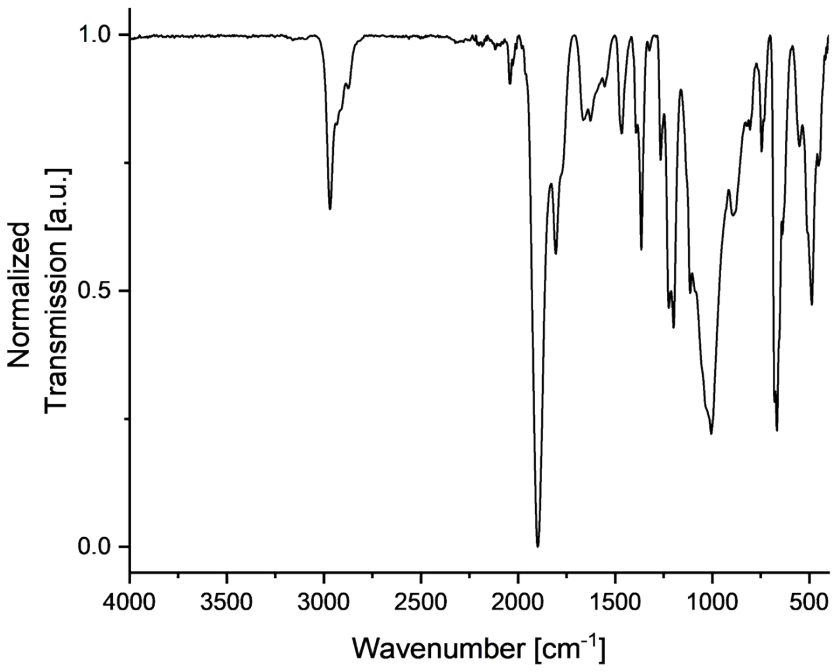

Figure S8. IR spectra of compound $[Cr(CO)_3(tBu_2NHSi)_3]$ (**1**).

[Mo(*t*Bu$_2$NHSi)$_3$(CO)$_3$] (2)

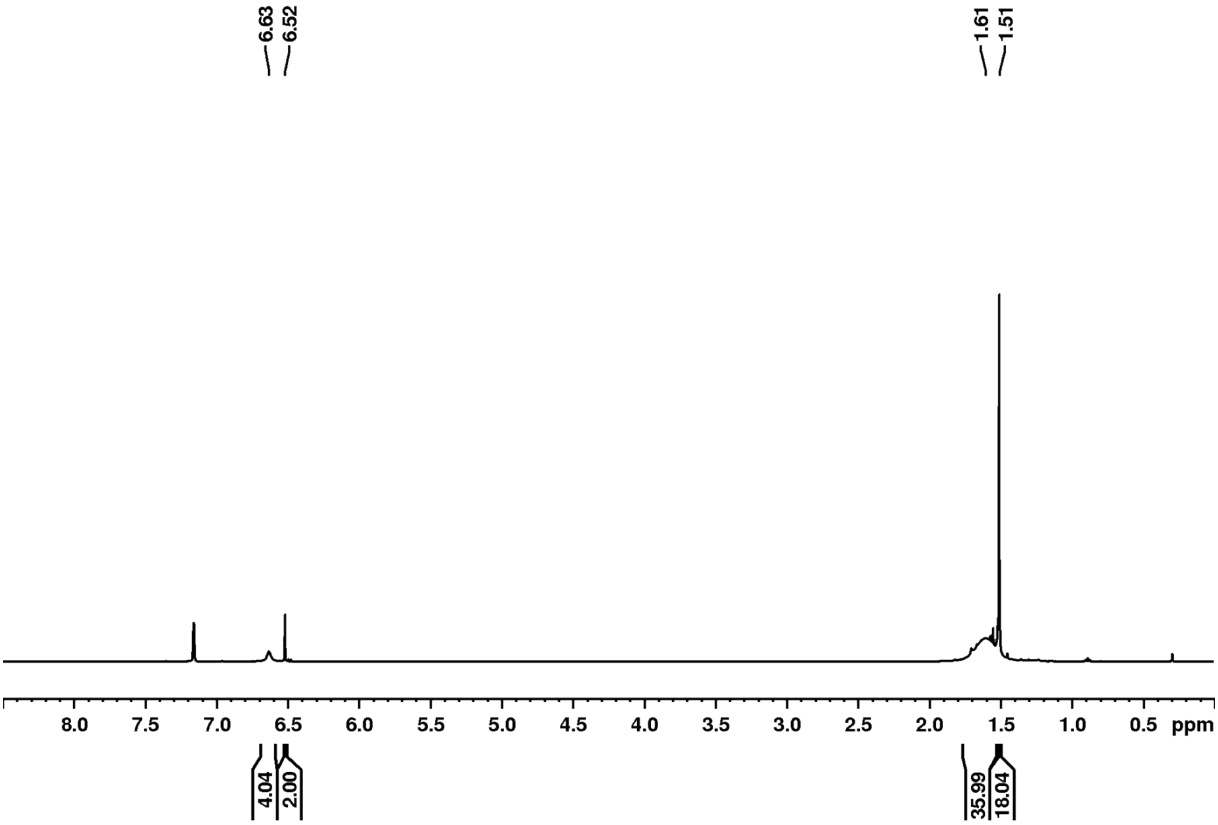

Figure S9. ^{1}H NMR spectrum (400.1 MHz, C_6D_6, 298 K) of [Mo(*t*Bu$_2$NHSi)$_3$(CO)$_3$] (**2**).

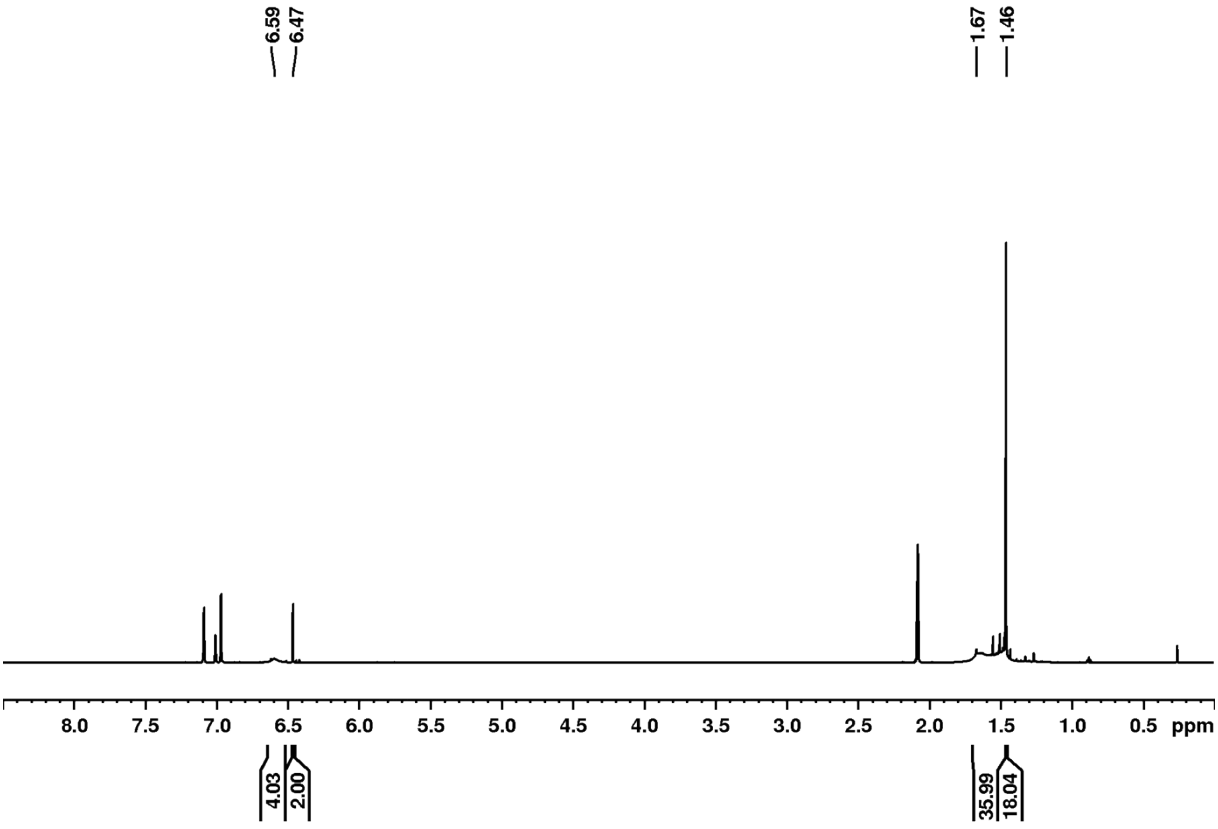

Figure S10. ^{1}H NMR spectrum (600.2 MHz, d_8-toluene, 298 K) of [Mo(*t*Bu$_2$NHSi)$_3$(CO)$_3$] (**2**).

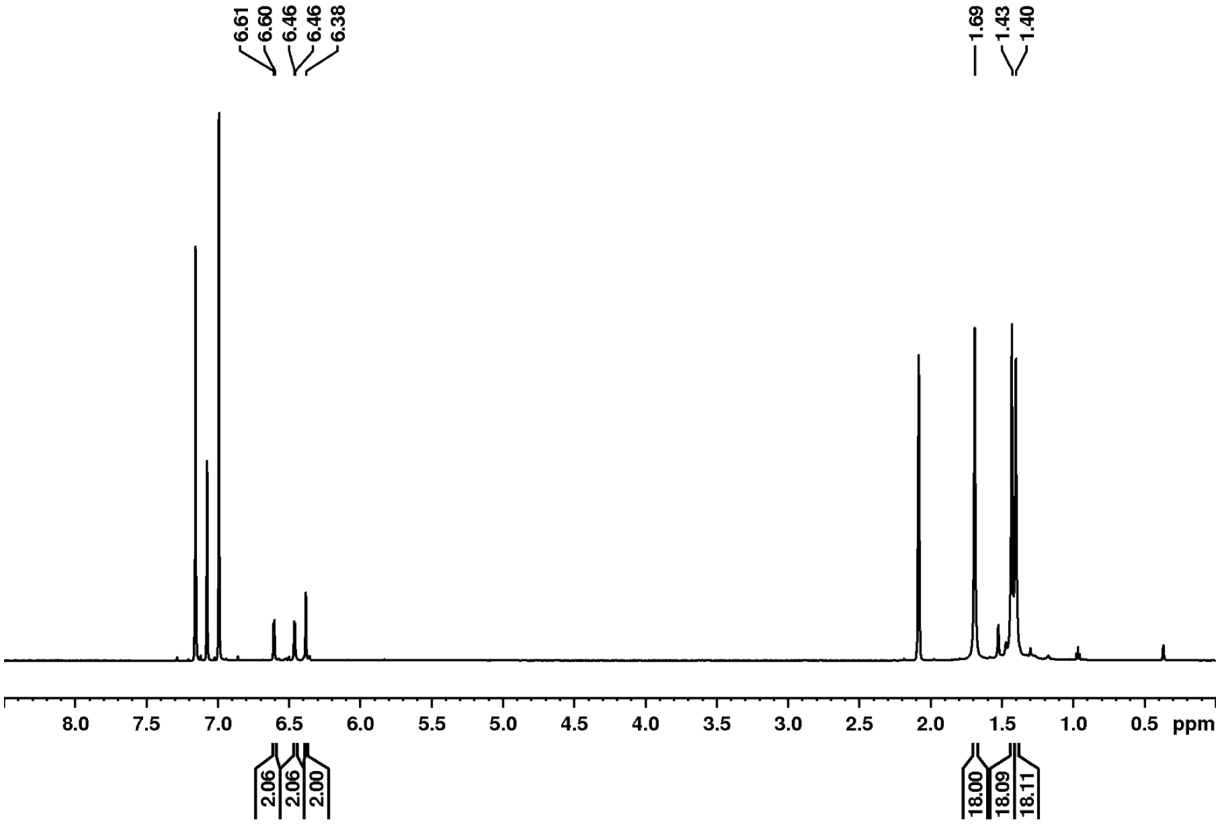

Figure S11. ^{1}H NMR spectrum (600.2 MHz, d_8-toluene, 193 K) of [Mo(*t*Bu$_2$NHSi)$_3$(CO)$_3$] (**2**).

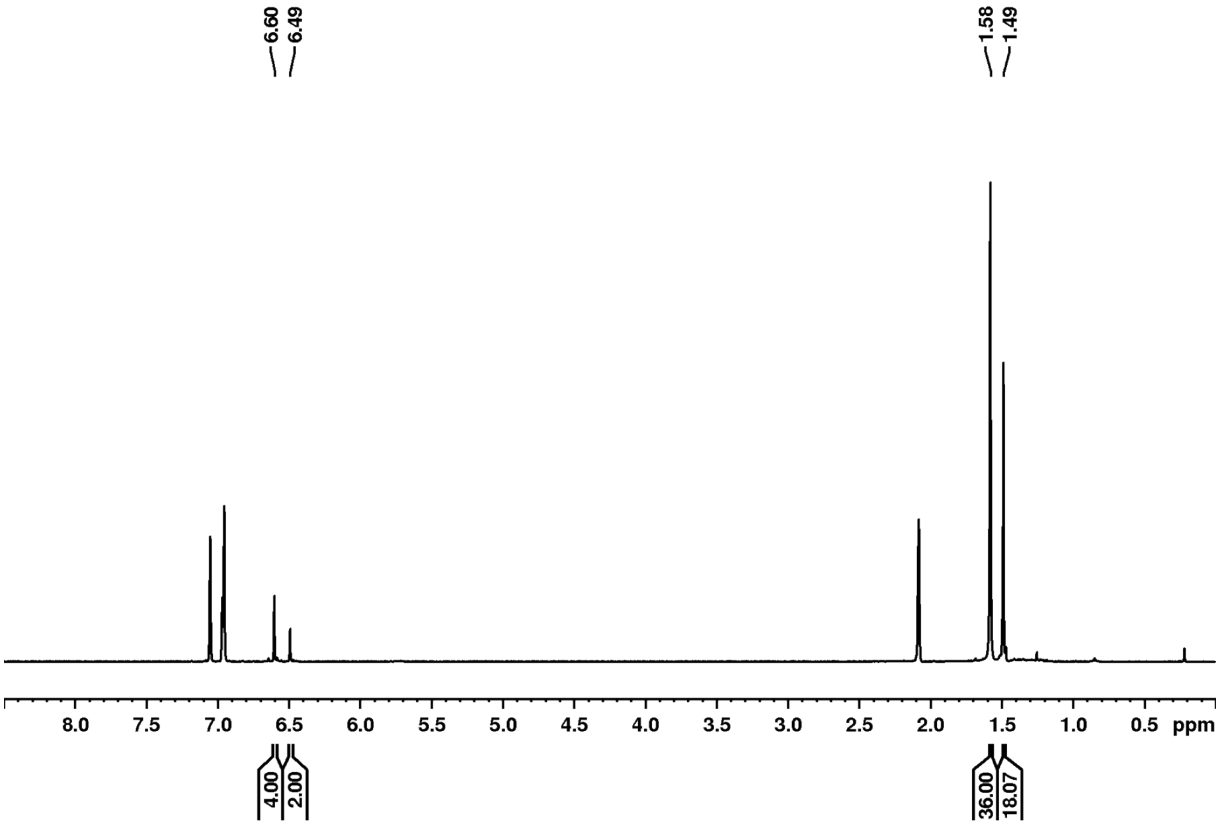

Figure S12. ^{1}H NMR spectrum (600.2 MHz, d_8-toluene, 373 K) of [Mo(*t*Bu$_2$NHSi)$_3$(CO)$_3$] (**2**).

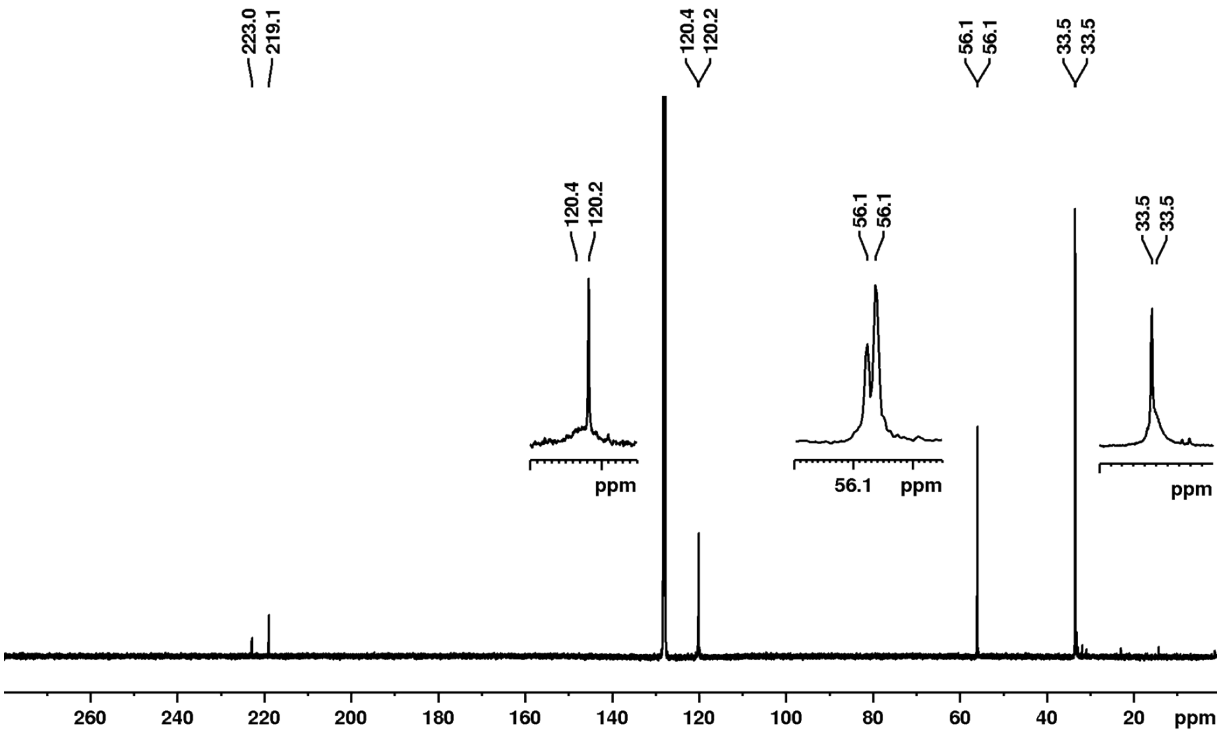

Figure S13. $^{13}C\{^{1}H\}$ NMR spectrum (100.6 MHz, C_6D_6, 298 K) of [Mo(*t*$Bu_2NHSi)_3(CO)_3$] (**2**).

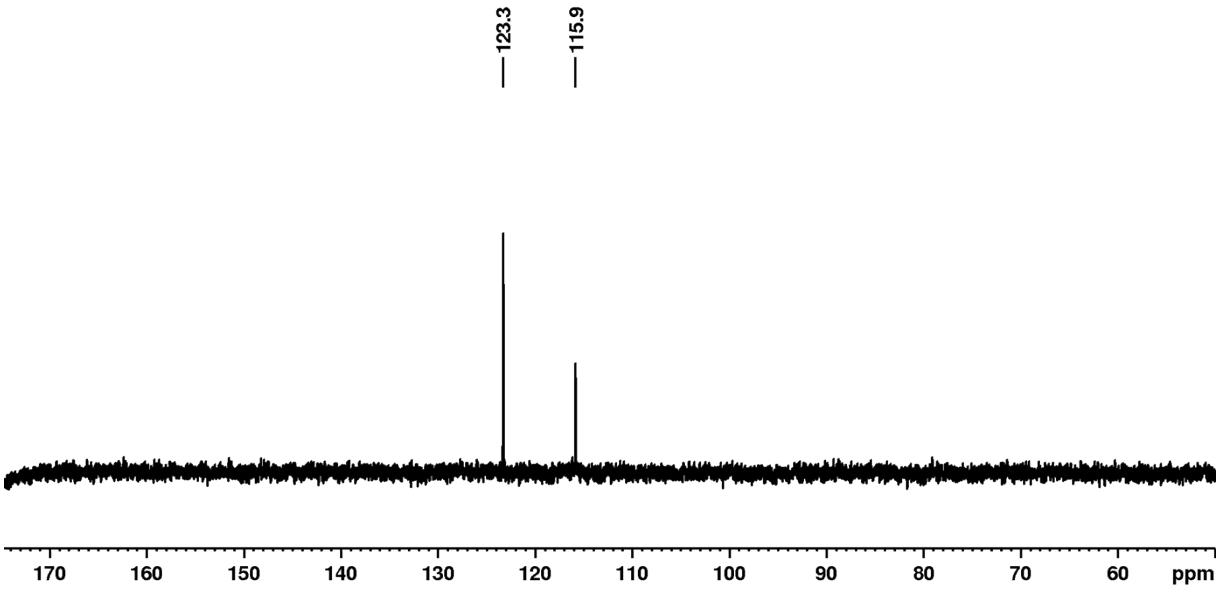

Figure S14. $^{29}Si\{^{1}H\}$ NMR spectrum (79.5 MHz, C_6D_6, 298 K) of [Mo(*t*$Bu_2NHSi)_3(CO)_3$] (**2**).

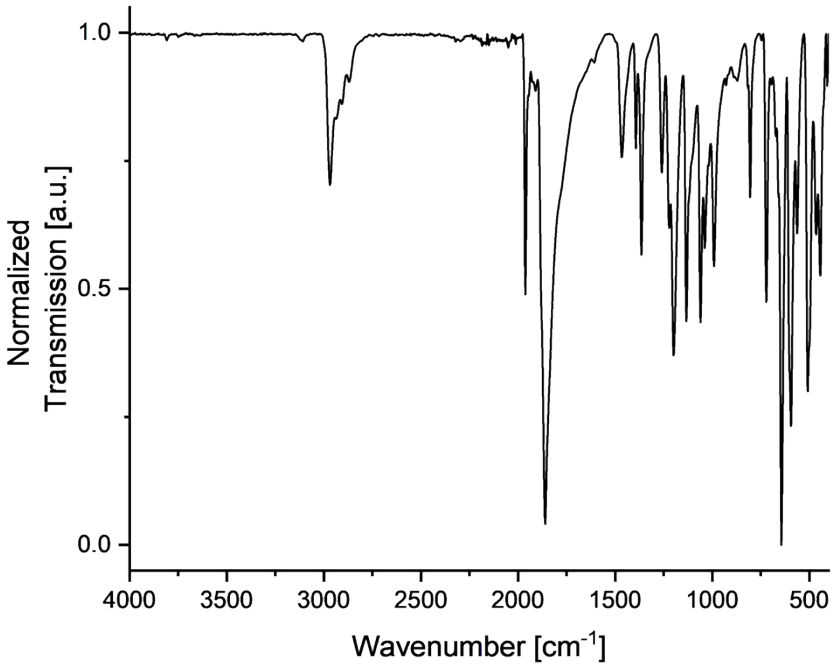

Figure S15. IR spectra of compound $[Mo(CO)_3(tBu_2NHSi)_3]$ (**2**).

$[Mo(Mes_2NHSi)_3(CO)_3]$ (3)

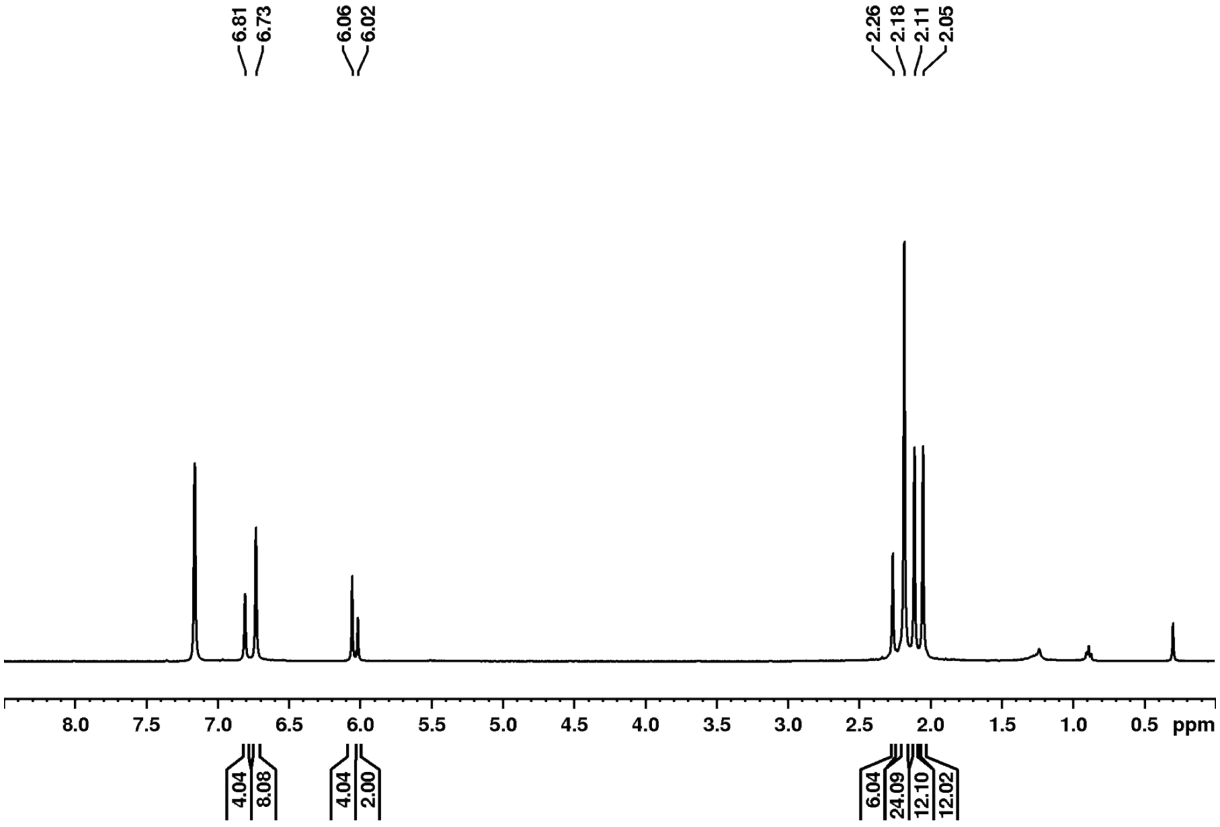

Figure S16. ^1H NMR spectrum (400.1 MHz, C_6D_6, 298 K) of $[Mo(Mes_2NHSi)_3(CO)_3]$ (**3**).

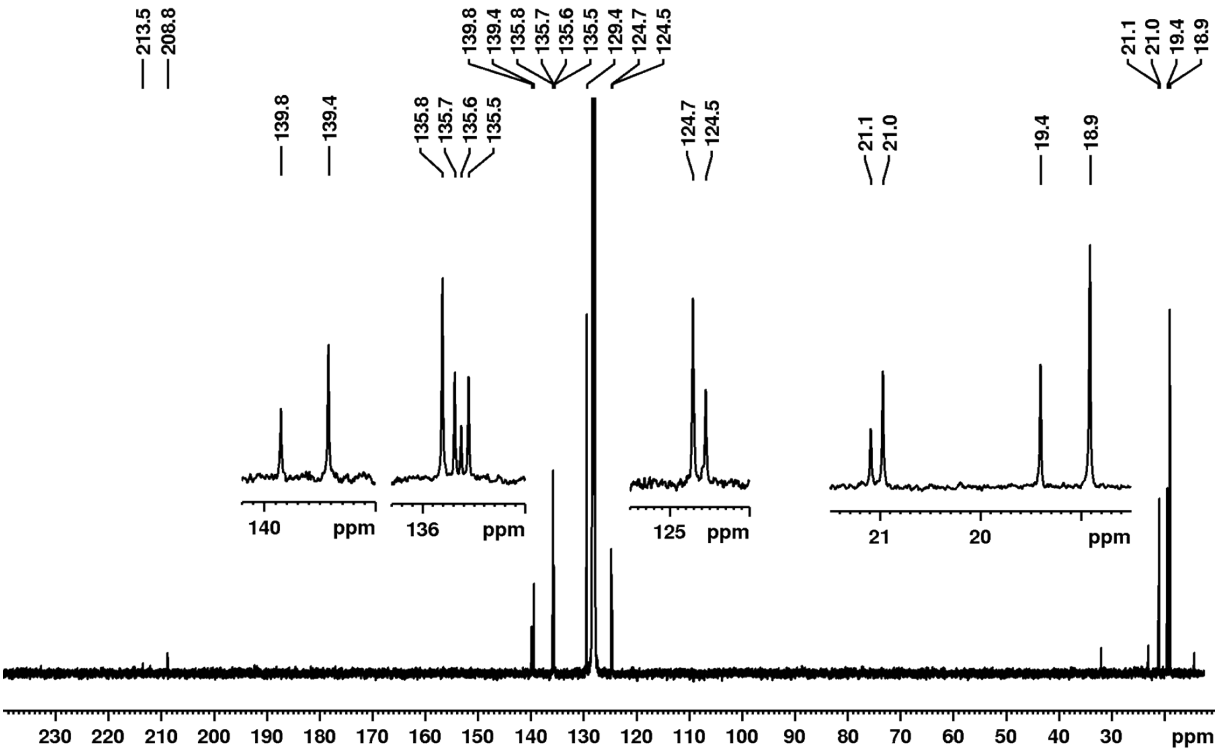

Figure S17. $^{13}C\{^{1}H\}$ NMR spectrum (100.6 MHz, C_6D_6, 298 K) of $[Mo(Mes_2NHSi)_3(CO)_3]$ (**3**) with minimal residues of *n*-hexane.

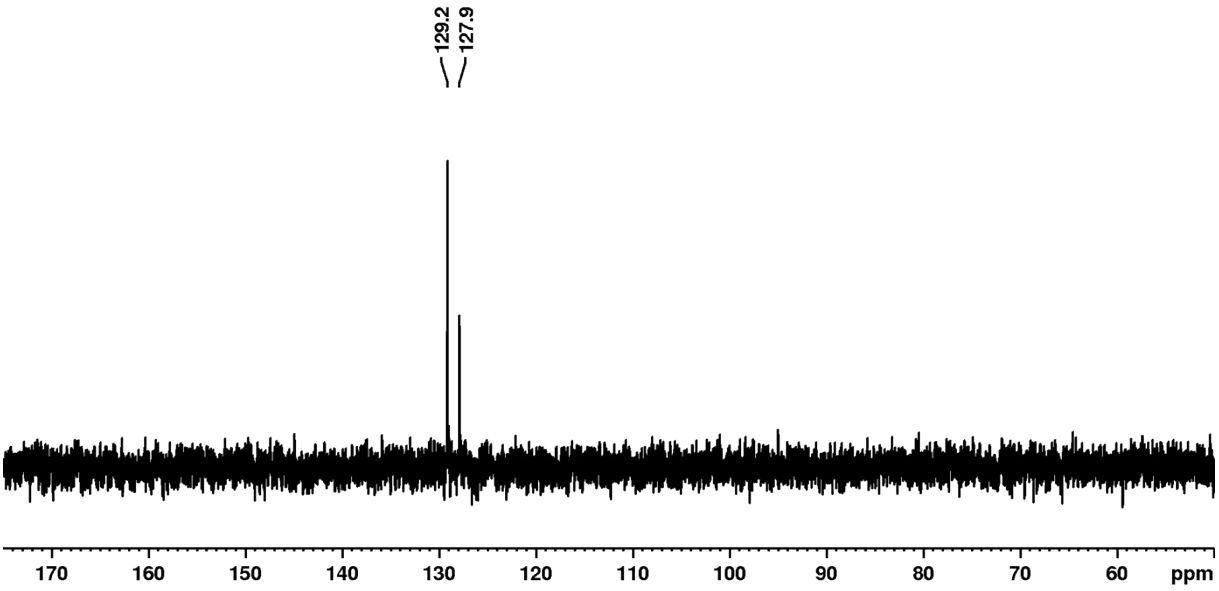

Figure S18. $^{29}Si\{^{1}H\}$ NMR spectrum (79.5 MHz, C_6D_6, 298 K) of $[Mo(Mes_2NHSi)_3(CO)_3]$ (**3**).

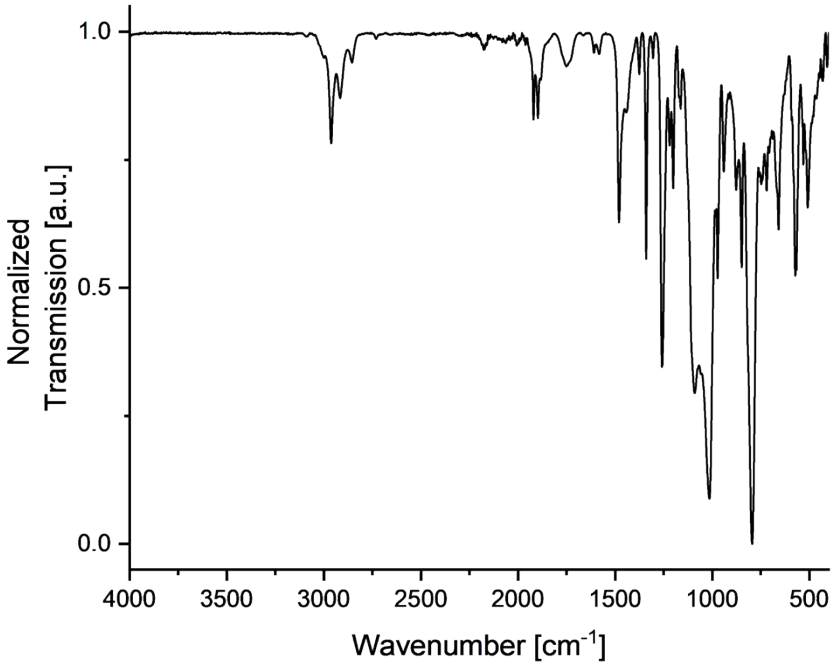

Figure S19. IR spectra of compound $[Mo(CO)_3(Mes_2NHSi)_3]$ (**3**).

$[Cr(CO)_3(Mes_2NHSi)_2(MeCN)]$ (4)

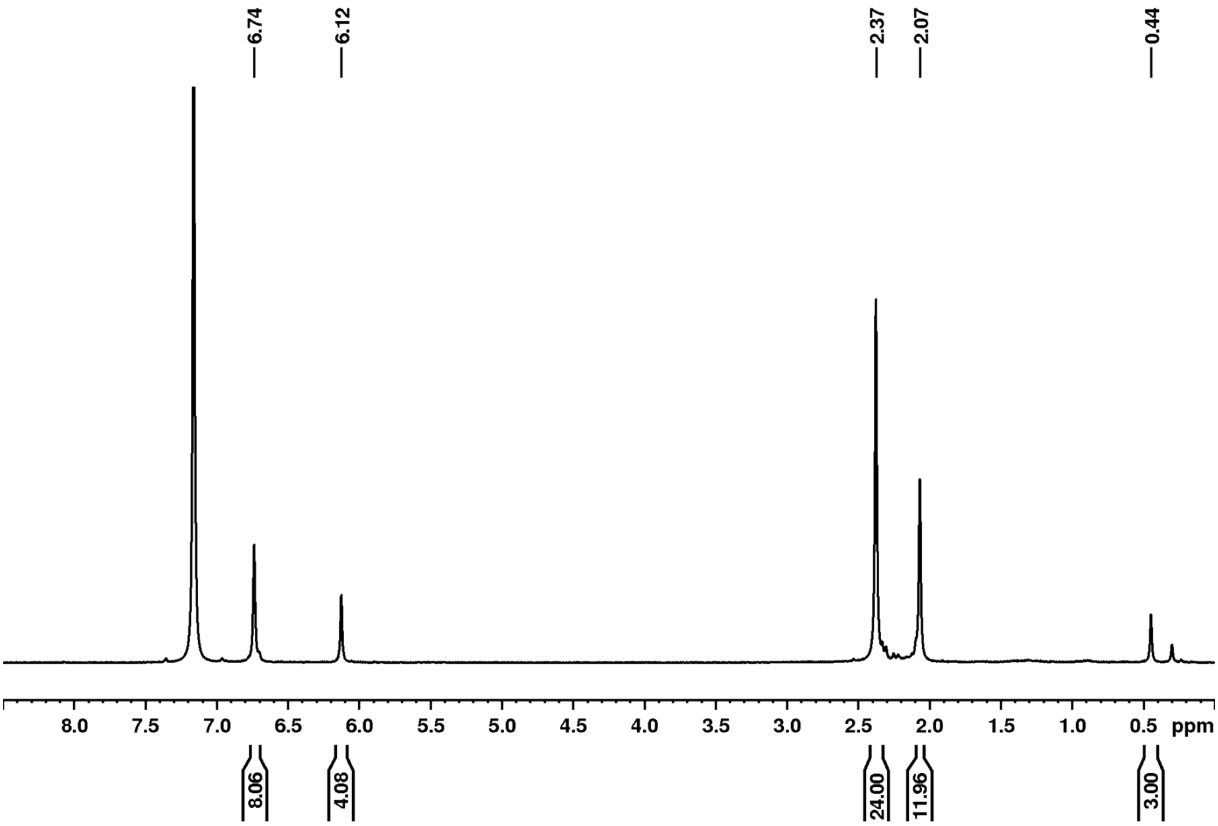

Figure S20. ^1H NMR spectrum (400.1 MHz, C_6D_6, 298 K) of $[Cr(CO)_3(Mes_2NHSi)_2(MeCN)]$ (**4**).

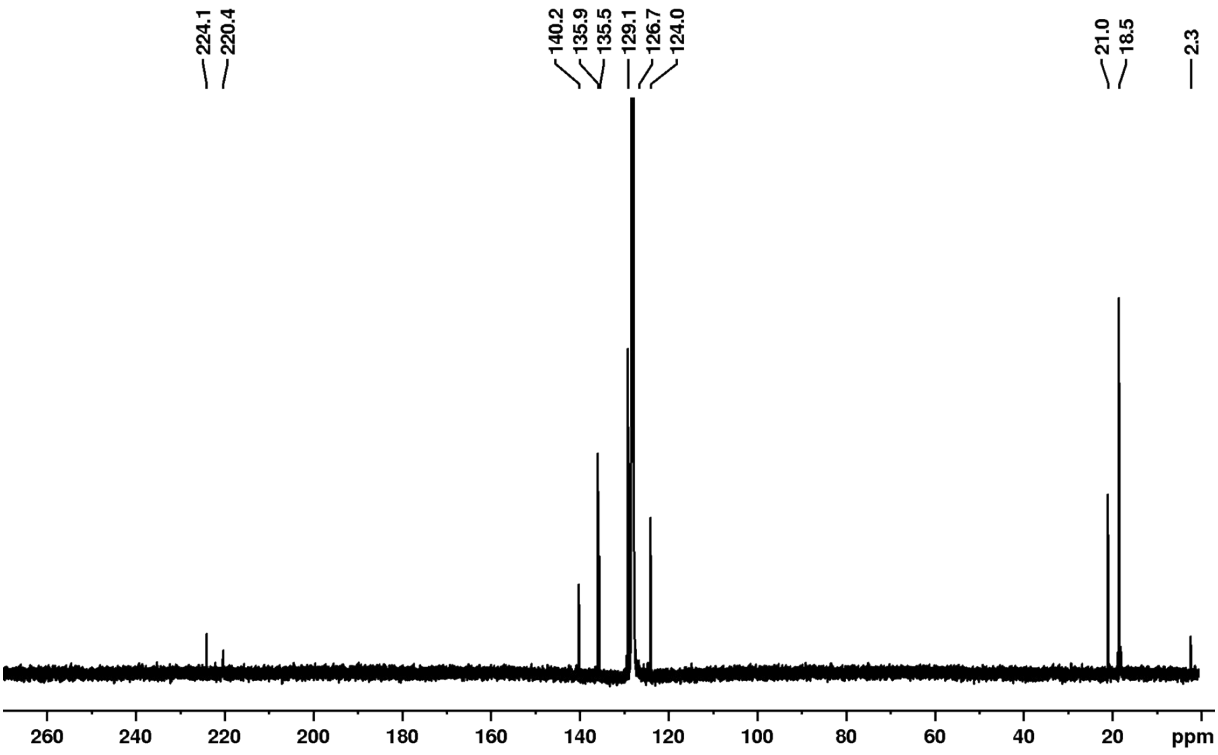

Figure S21. $^{13}C\{^{1}H\}$ NMR spectrum (100.6 MHz, C_6D_6, 298 K) of $[Cr(CO)_3(Mes_2NHSi)_2(MeCN)]$ (**4**).

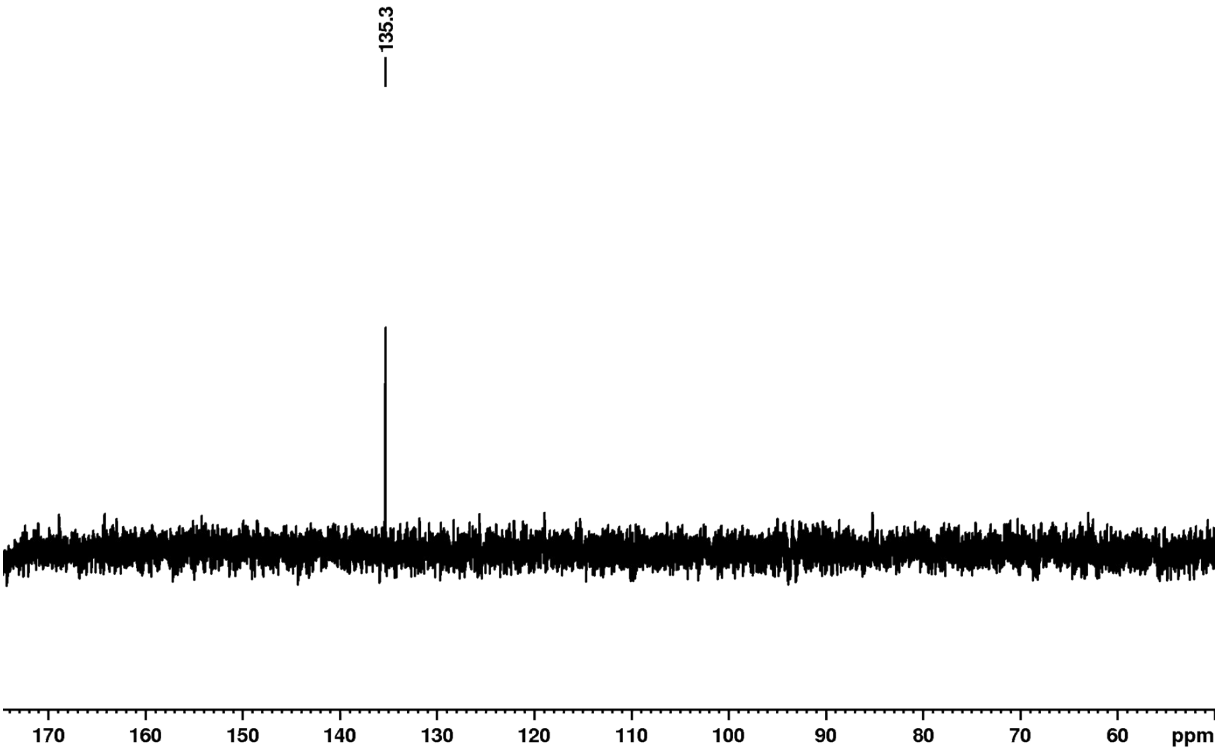

Figure S22. $^{29}Si\{^{1}H\}$ NMR spectrum (79.5 MHz, C_6D_6, 298 K) of $[Cr(CO)_3(Mes_2NHSi)_2(MeCN)]$ (**4**).

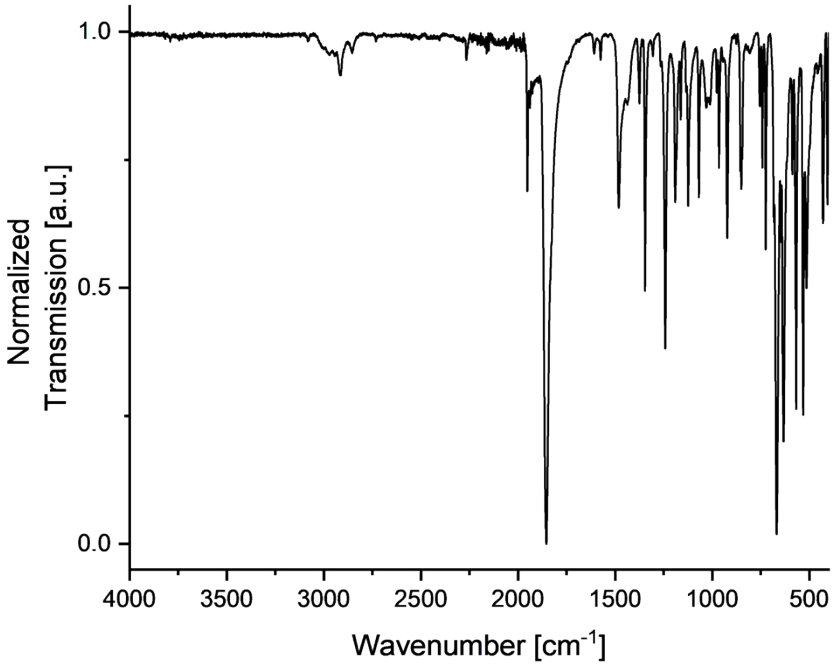

Figure S23. IR spectra of compound $[Cr(CO)_3(Mes_2NHSi)_2(NCMe)]$ (**4**).

$[Mo(Dipp_2NHSi)_2(CO)_3(MeCN)]$ (5)

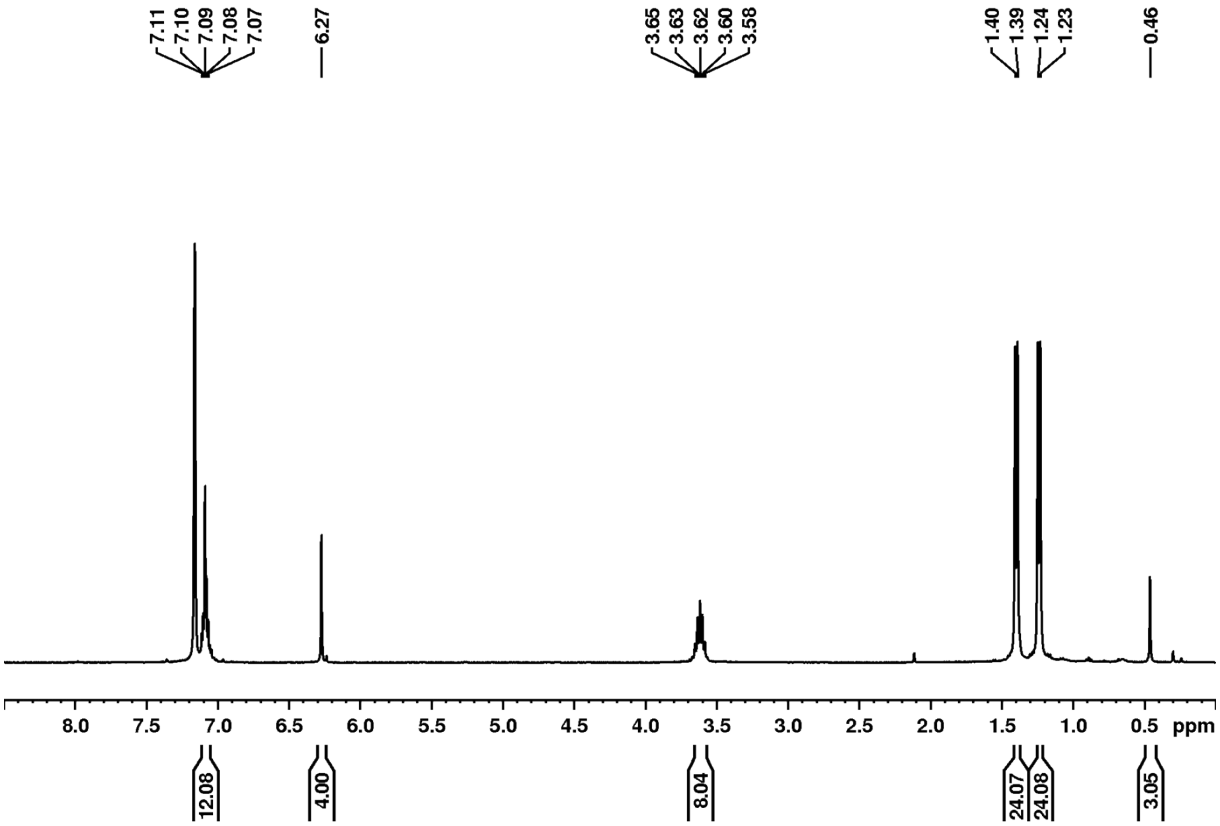

Figure S24. ^1H NMR spectrum (400.1 MHz, C_6D_6, 298 K) of $[Mo(Dipp_2NHSi)_2(CO)_3(MeCN)]$ (**5**).

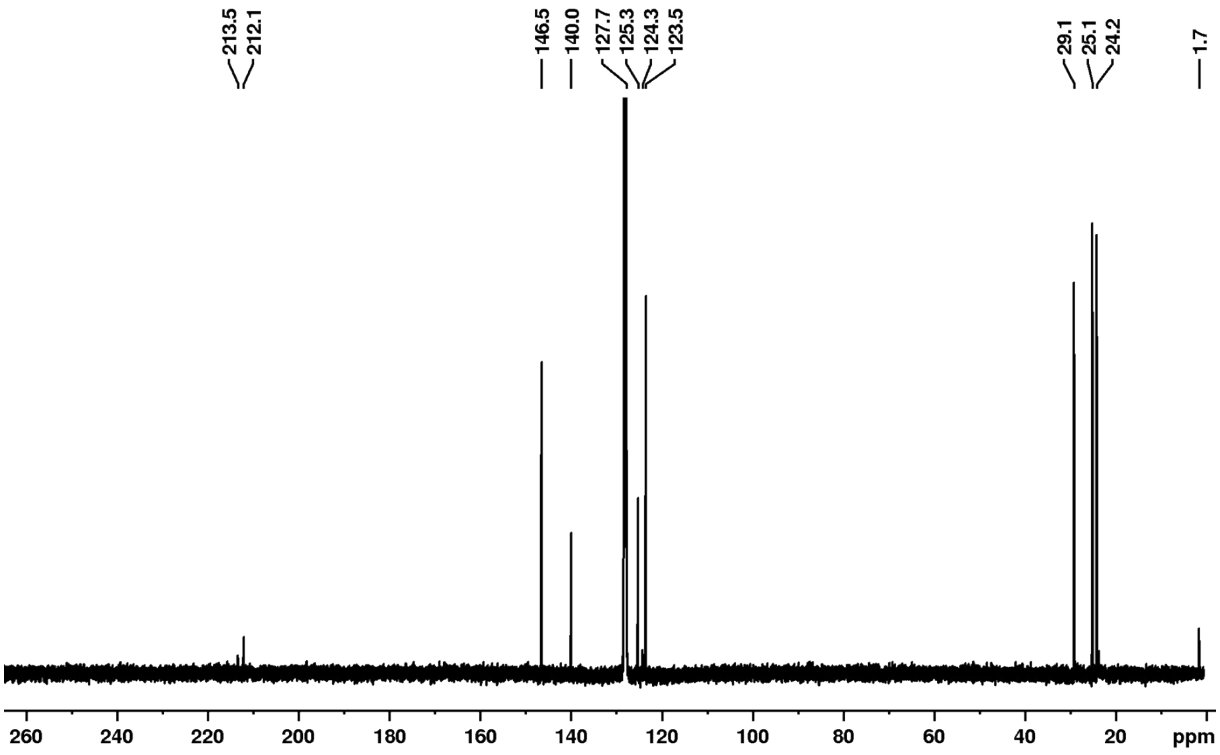

Figure S25. $^{13}C\{^{1}H\}$ NMR spectrum (100.6 MHz, C_6D_6, 298 K) of $[Mo(Dipp_2NHSi)_2(CO)_3(MeCN)]$ (**5**).

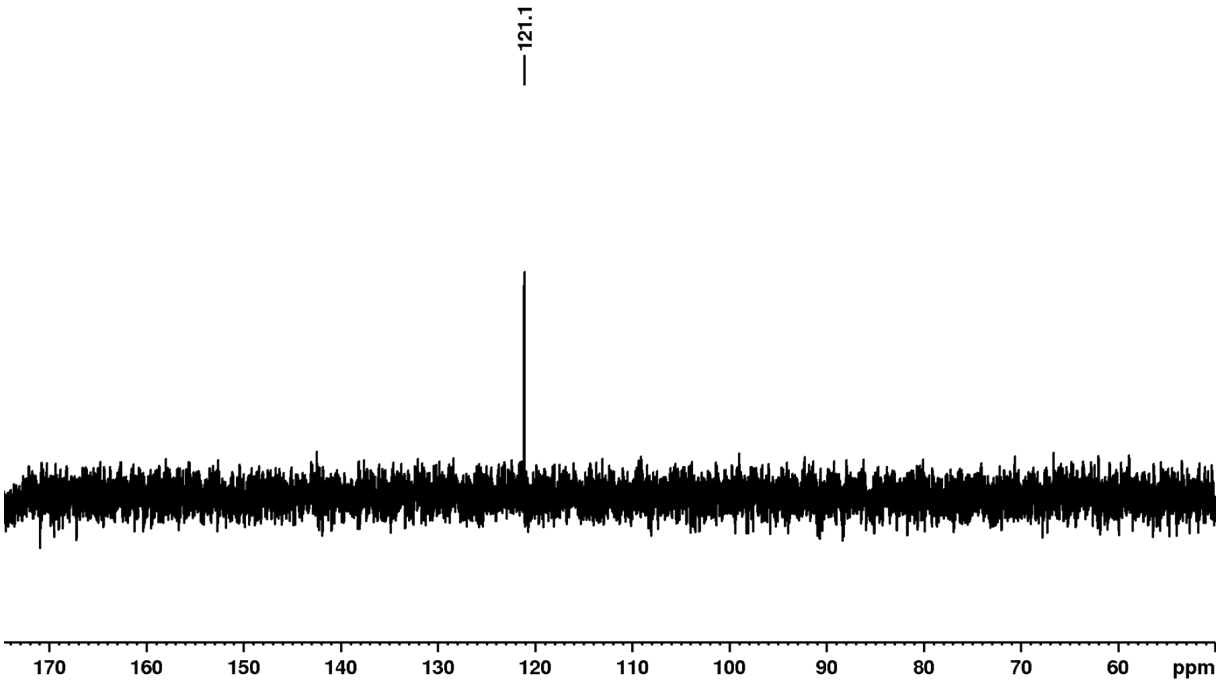

Figure S26. $^{29}Si\{^{1}H\}$ NMR spectrum (79.5 MHz, C_6D_6, 298 K) of $[Mo(Dipp_2NHSi)_2(CO)_3(MeCN)]$ (**5**).

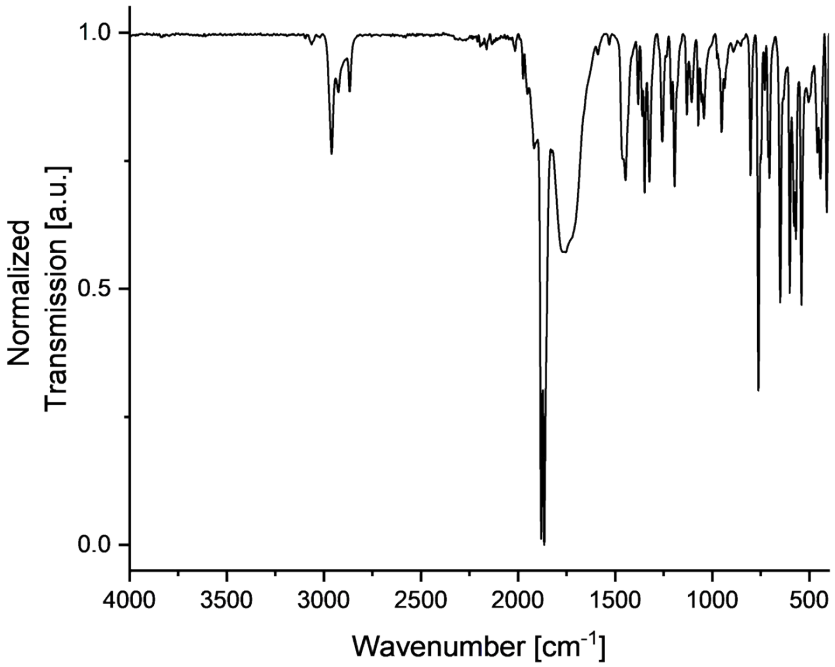

Figure S27. IR spectra of compound $[Mo(CO)_3(Dipp_2NHSi)_2(NCMe)]$ (**5**).

$[Cr(CO)_3(Mes_2NHSi)_2(py)]$ (6)

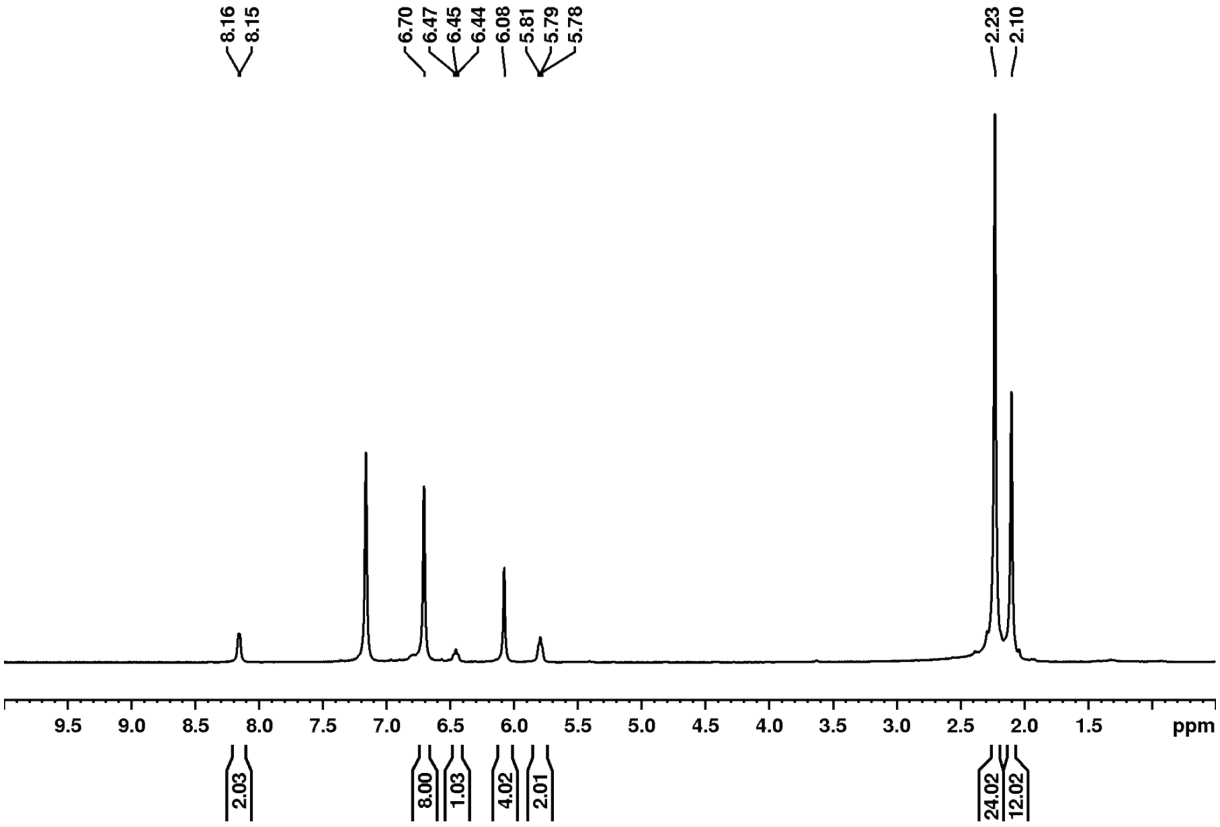

Figure S28. ^1H NMR spectrum (400.1 MHz, C_6D_6, 298 K) of $[Cr(CO)_3(Mes_2NHSi)_2(py)]$ (**6**).

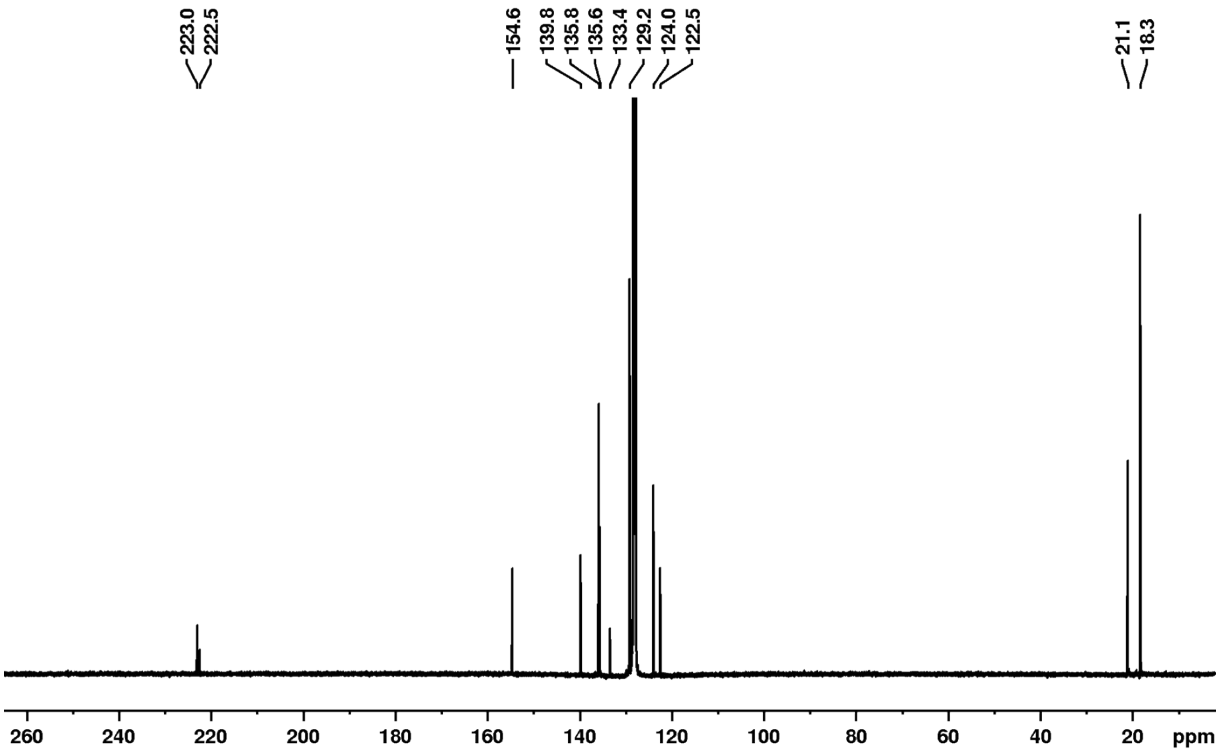

Figure S29. $^{13}C\{^{1}H\}$ NMR spectrum (100.6 MHz, C_6D_6, 298 K) of $[Cr(CO)_3(Mes_2NHSi)_2(py)]$ (**6**).

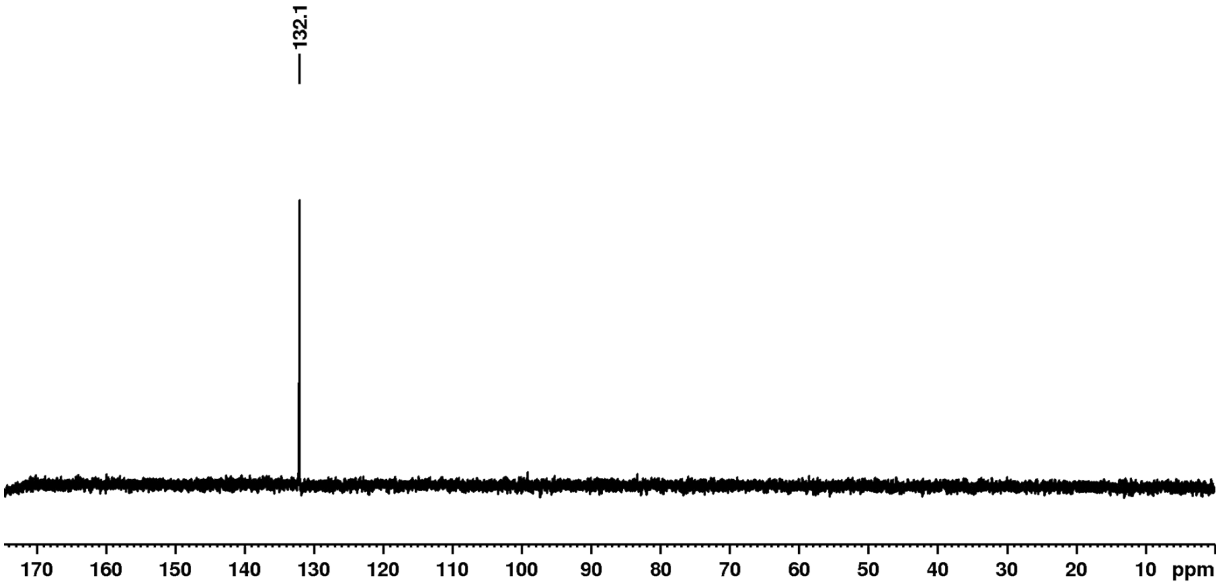

Figure S30. $^{29}Si\{^{1}H\}$ NMR spectrum (79.5 MHz, C_6D_6, 298 K) of $[Cr(CO)_3(Mes_2NHSi)_2(py)]$ (**6**).

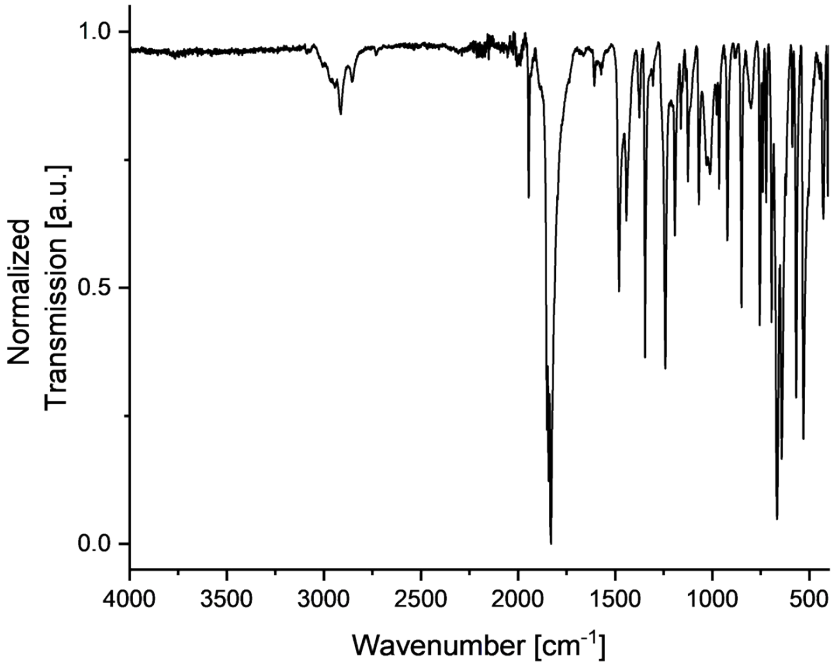

Figure S31. IR spectra of compound $[Cr(CO)_3(Mes_2NHSi)_2(py)]$ (**6**).

$[Cr(CO)_3(Mes_2NHSi)_2(DMAP)]$ (7)

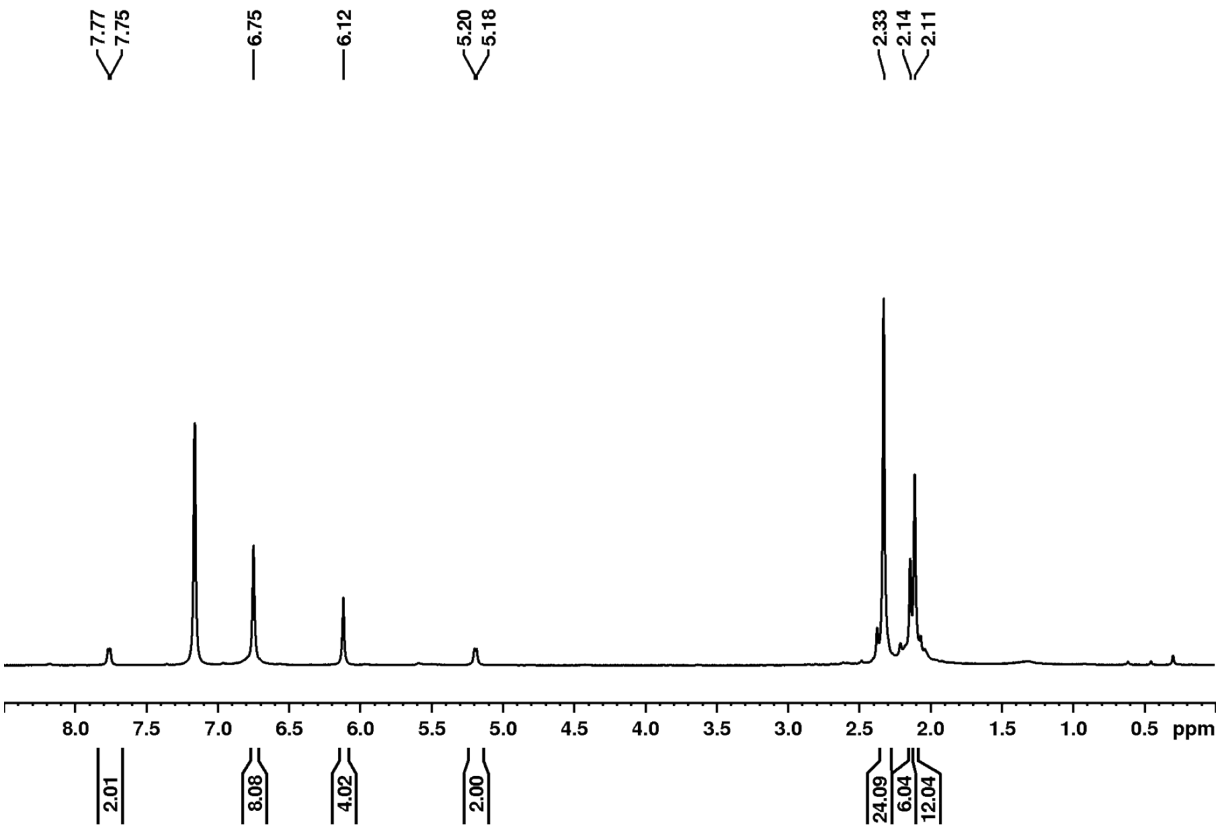

Figure S32. ^1H NMR spectrum (400.1 MHz, C_6D_6, 298 K) of $[Cr(CO)_3(Mes_2NHSi)_2(DMAP)]$ (**7**).

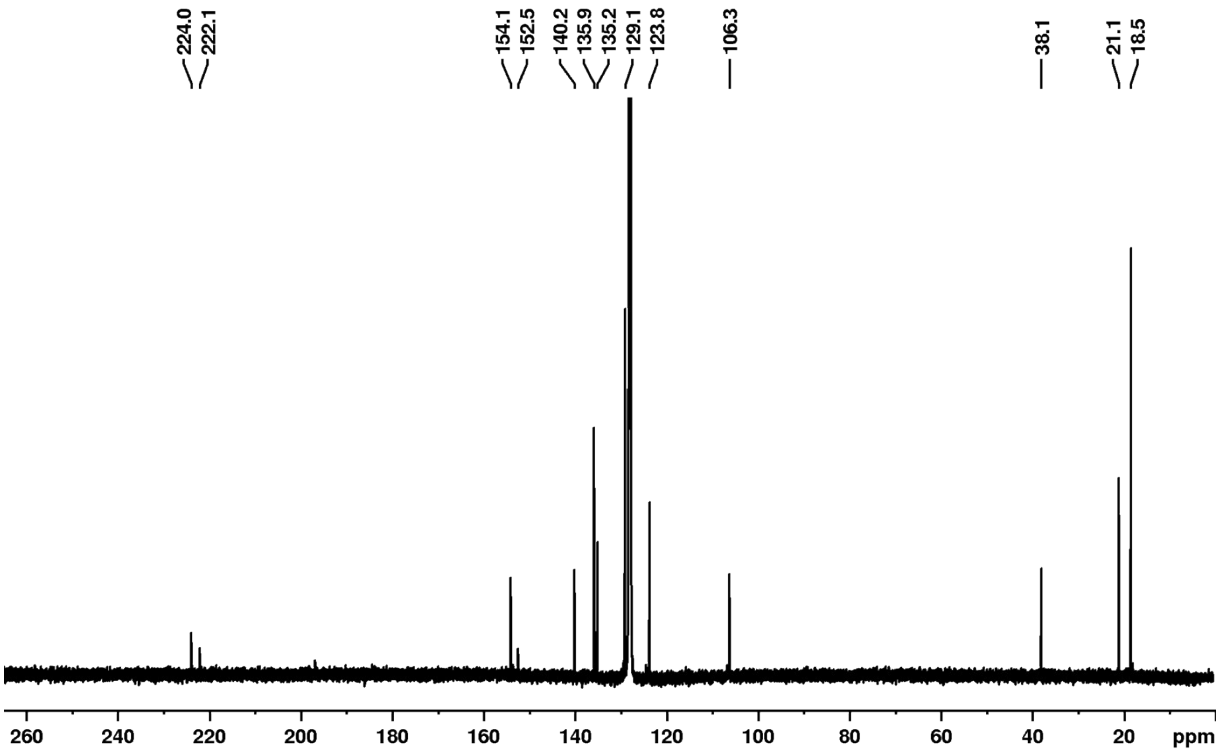

Figure S33. $^{13}C\{^{1}H\}$ NMR spectrum (100.6 MHz, C_6D_6, 298 K) of $[Cr(CO)_3(Mes_2NHSi)_2(DMAP)]$ (**7**).

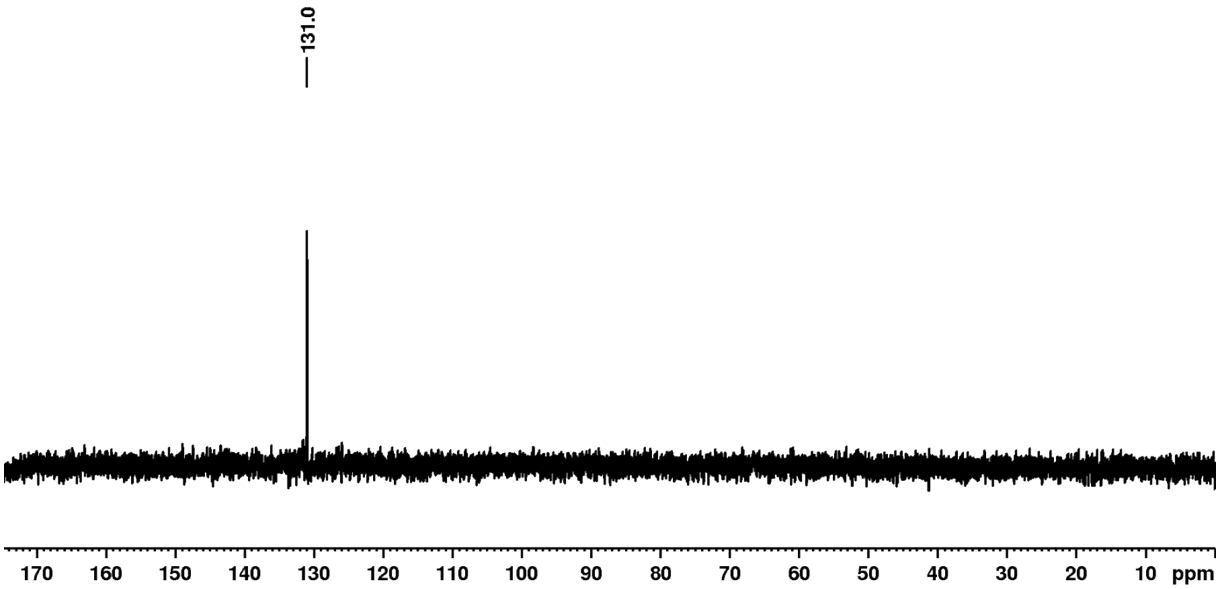

Figure S34. $^{29}Si\{^{1}H\}$ NMR spectrum (79.5 MHz, C_6D_6, 298 K) of $[Cr(CO)_3(Mes_2NHSi)_2(DMAP)]$ (**7**).

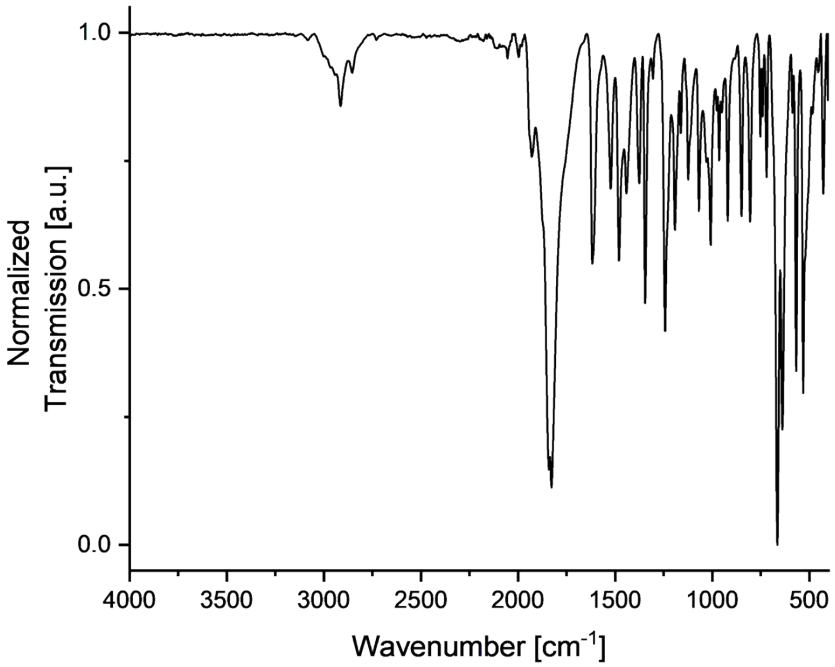

Figure S35. IR spectra of compound $[Cr(CO)_3(Mes_2NHSi)_2(DMAP)]$ (**7**).

$[Cr(CO)_3(Mes_2NHSi)_2(CN\text{-}tBu)]$ (8)

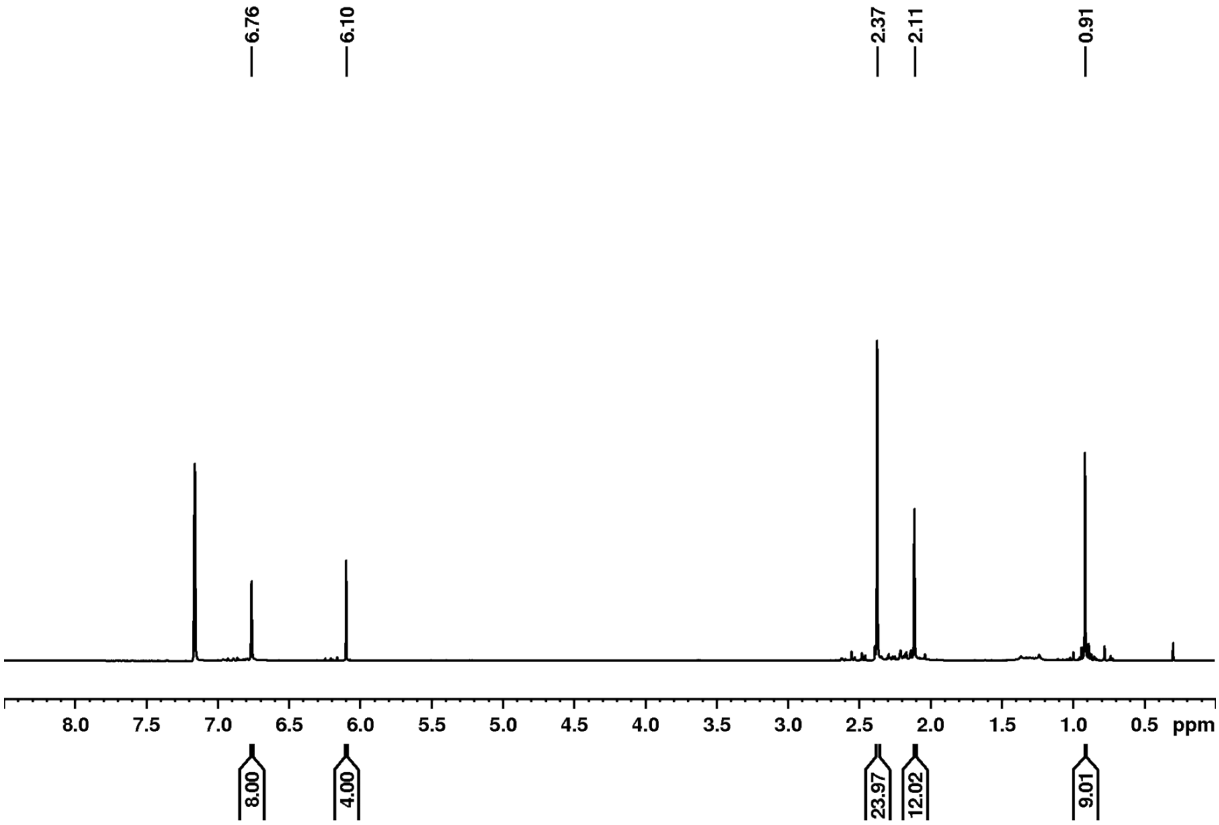

Figure S36. ^1H NMR spectrum (400.1 MHz, C_6D_6, 298 K) of $[Cr(CO)_3(Mes_2NHSi)_2(CN\text{-}tBu)]$ (**8**).

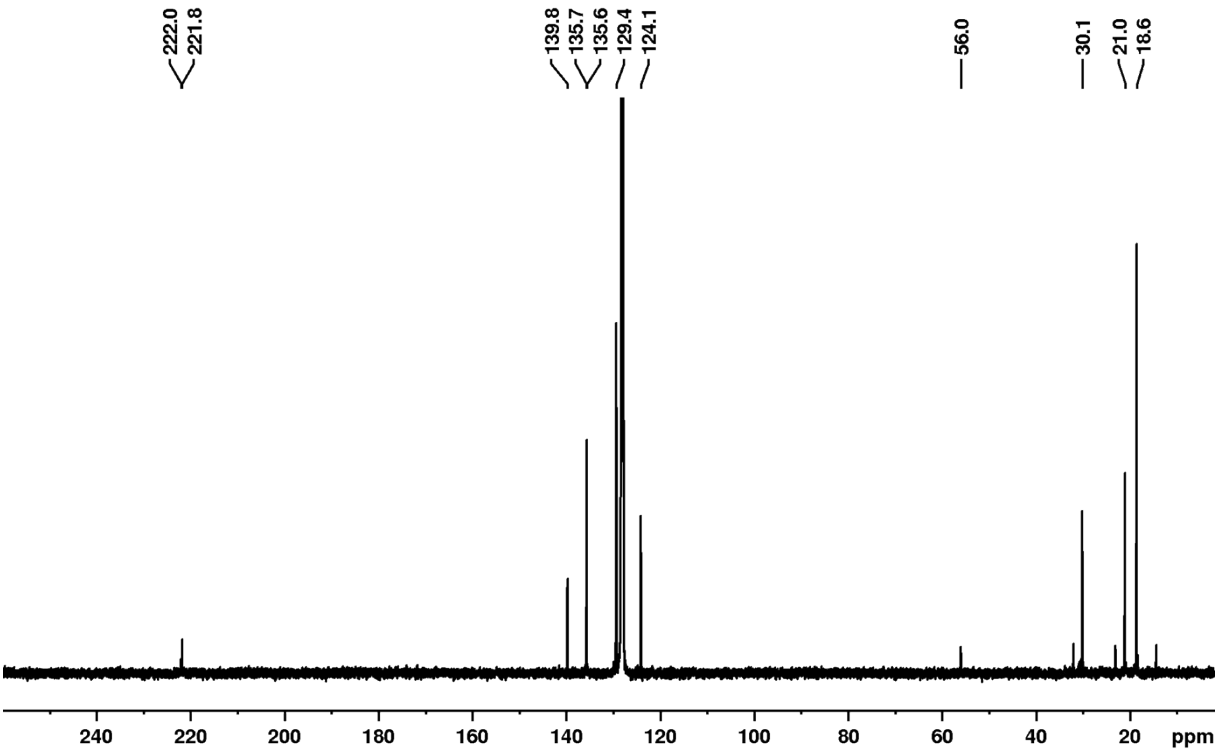

Figure S37. $^{13}C\{^{1}H\}$ NMR spectrum (100.6 MHz, C_6D_6, 298 K) of $[Cr(CO)_3(Mes_2NHSi)_2(CN\text{-}t\text{Bu})]$ (**8**).

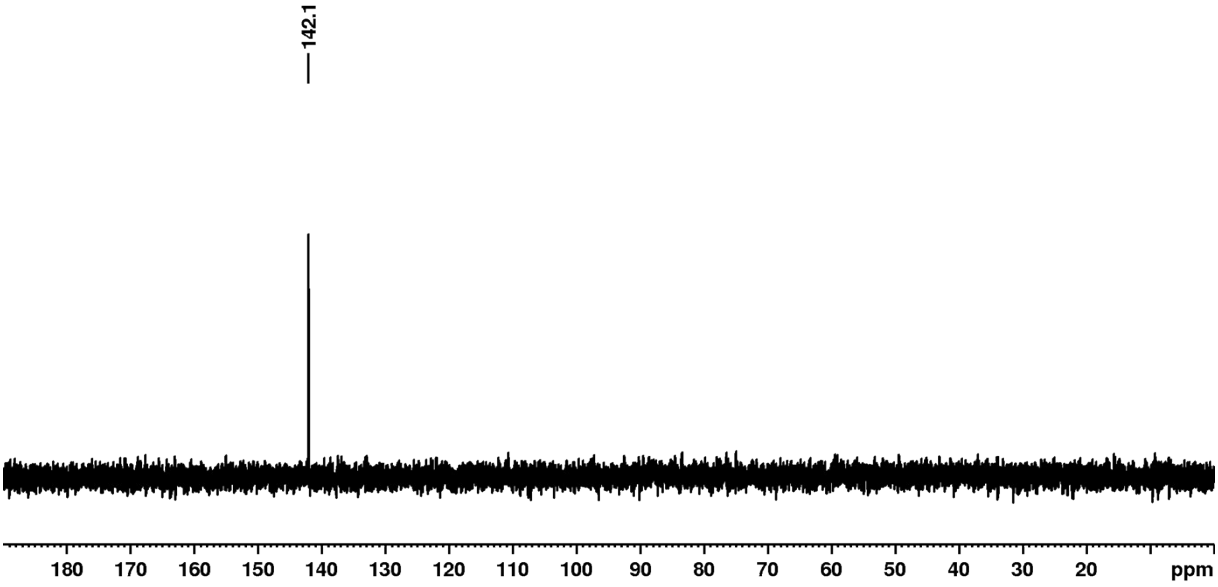

Figure S38. $^{29}Si\{^{1}H\}$ NMR spectrum (79.5 MHz, C_6D_6, 298 K) of $[Cr(CO)_3(Mes_2NHSi)_2(CN\text{-}t\text{Bu})]$ (**8**).

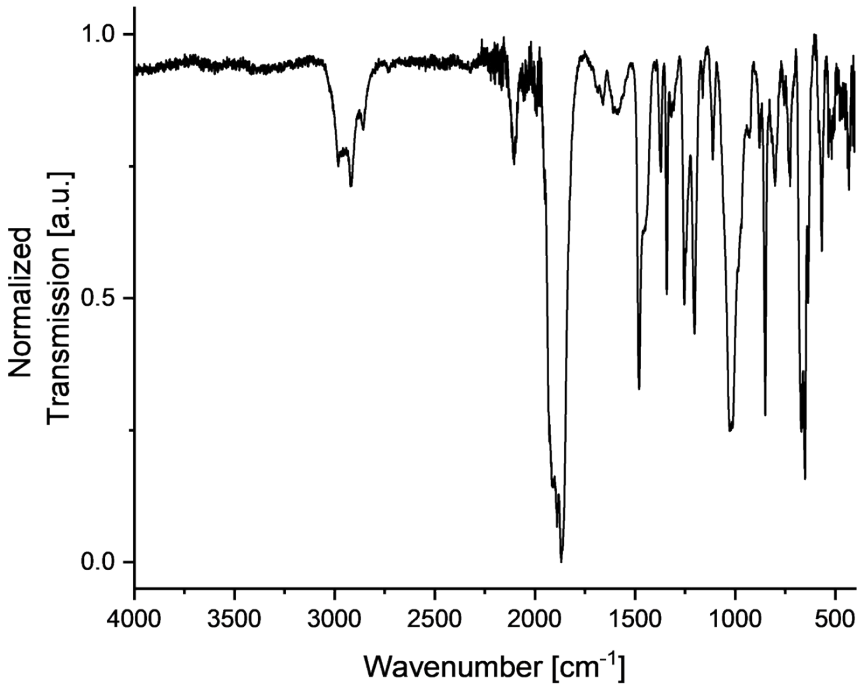

Figure S39. IR spectra of compound $[Cr(CO)_3(Mes_2NHSi)_2(CN\textit{t}Bu)]$ (**8**).

$[Cr(CO)_3(Mes_2NHSi)_2(IMe^{Me})]$ (9)

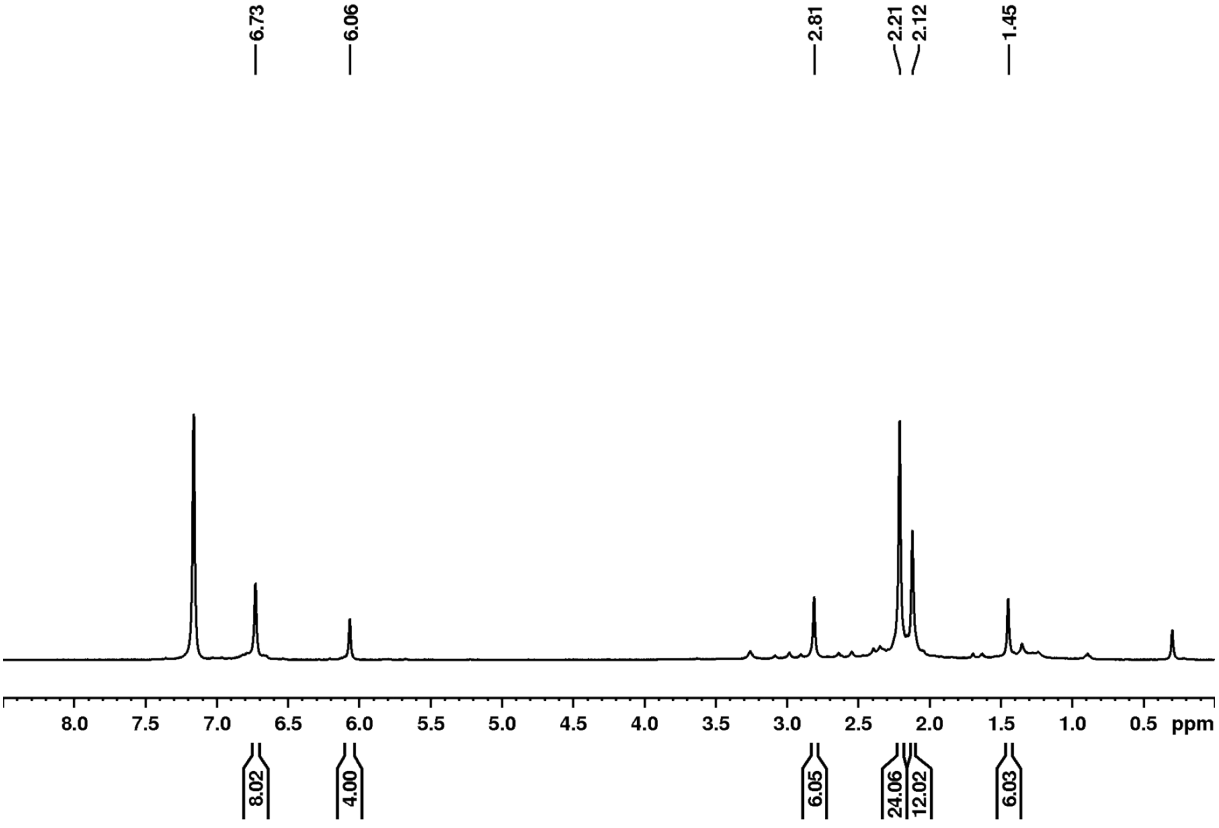

Figure S40. ^1H NMR spectrum (400.1 MHz, C_6D_6, 298 K) of $[Cr(CO)_3(Mes_2NHSi)_2(IMe_4)]$ (**9**).

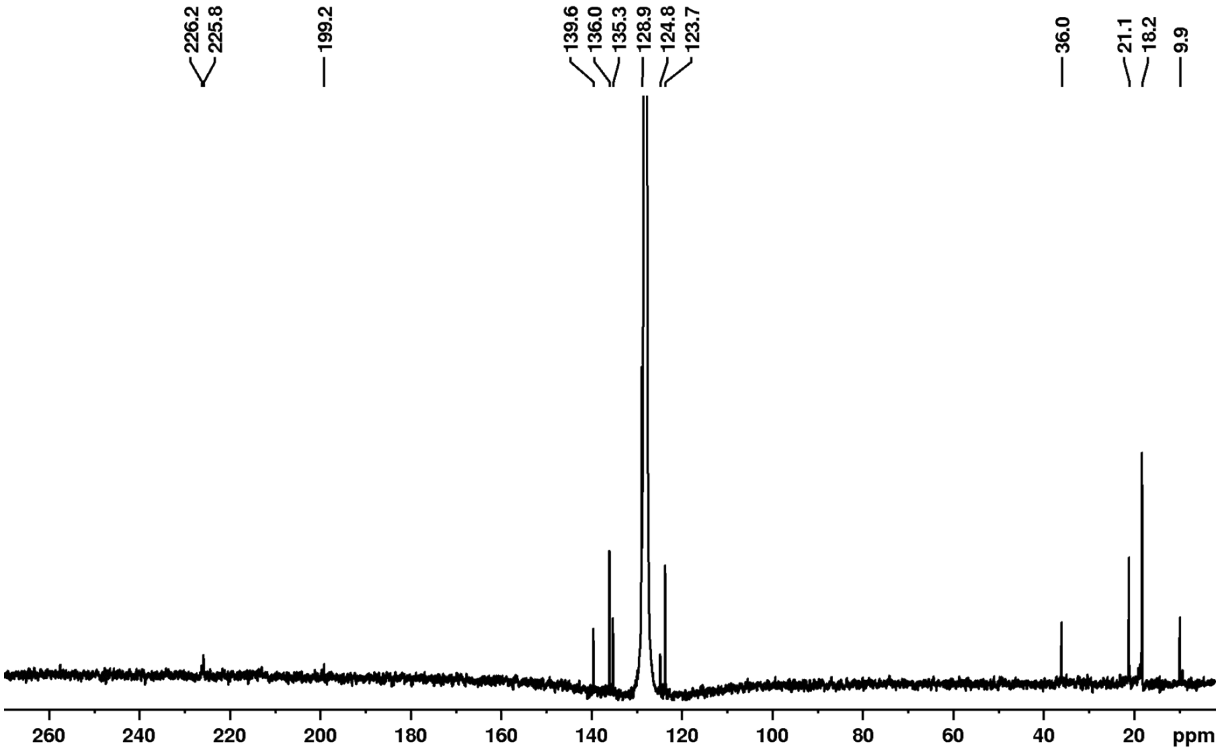

Figure S41. $^{13}C\{^{1}H\}$ NMR spectrum (100.6 MHz, C_6D_6, 298 K) of $[Cr(CO)_3(Mes_2NHSi)_2(IMe_4)]$ (**9**).

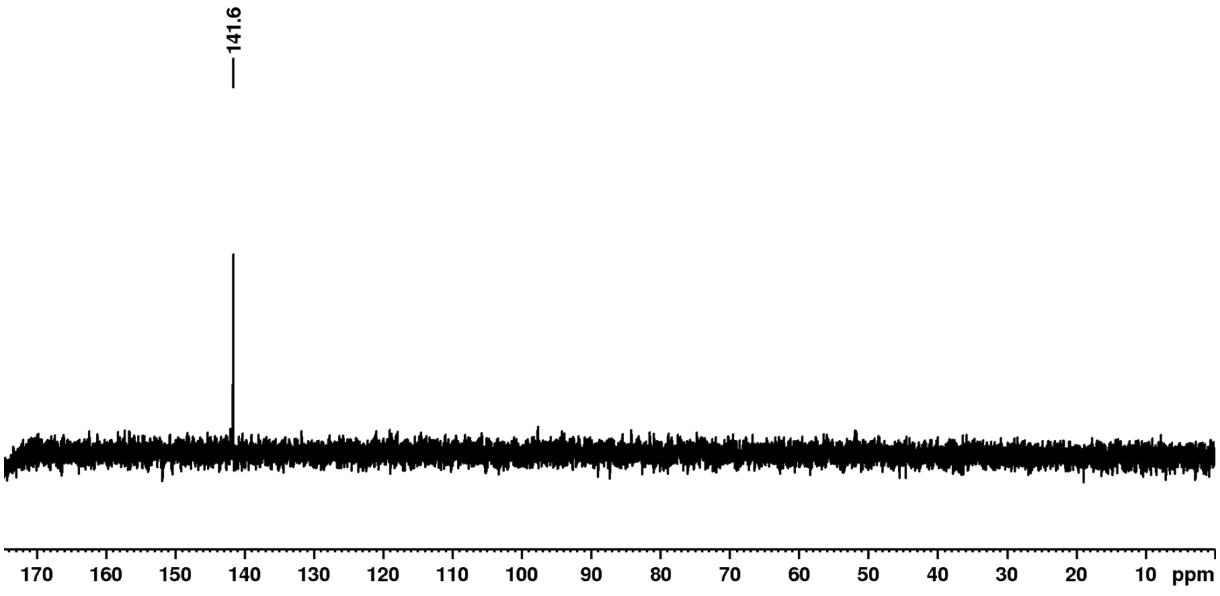

Figure S42. $^{29}Si\{^{1}H\}$ NMR spectrum (79.5 MHz, C_6D_6, 298 K) of $[Cr(CO)_3(Mes_2NHSi)_2(IMe_4)]$ (**9**).

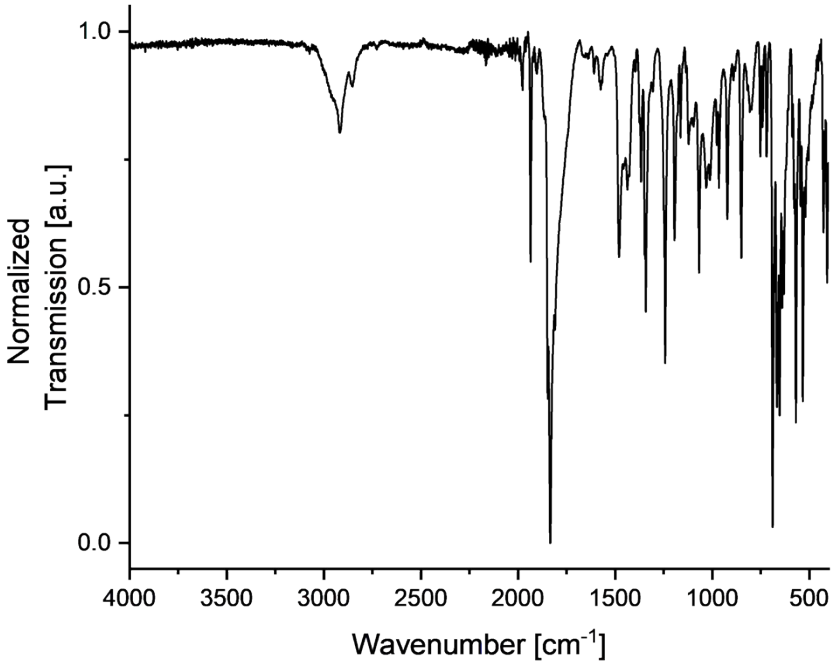

Figure S43. IR spectra of compound $[Cr(CO)_3(Mes_2NHSi)_2(IMe^{Me})]$ (**9**).

3) Calculation of barriers ΔG‡ from experimental NMR data

With the experimental data of the VT ^{1}H NMR spectra (T_c, Δv of the coalescence points) the activation energy barrier ΔG‡ for the processes were calculated using following equation (J. Sandström, *Dynamic NMR spectroscopy*, Academic Press, **1982**):

$$\Delta G^{\ddagger} = 19.14\, T_c \left[log_{10}\left(\frac{T_c}{\Delta v}\right) + 10.319\right]$$

ΔG‡ = activation energy barrier (J/mol)

T_c = coalescence temperature in K

Δv = frequency difference of both signals in Hz

4) Crystallograohic Details

Crystal structure of $[Cr(CO)_3(tBu_2NHSi)_3]$ (1)

$C_{33}H_{60}Si_3N_6O_3Cr$, M_r = 725.14 g/mol, T = 99.99(10) K, λ = 1.54184 Å, colorless block, 0.03 × 0.14 × 0.21 mm^3, monoclinic, space group *C*2/c, a = 17.1775(3) Å, b = 10.9182(2) Å, c = 21.2108(4) Å, α = 90 °, β = 100.770(2) °, γ = 90 °, V = 3907.96(13) $Å^3$, Z = 4, ρ_{calcd} = 1.232 Mg/m^3, μ = 3.599 mm^{-1}, F(000) = 1560, 18888 reflections, –19 ≤ h ≤ 21, –13 ≤ k ≤ 11, –25 ≤ l ≤ 26, 4.243 ° < θ < 75.583 °, completeness 99.6 %, 3917 independent reflections, 3425 reflections observed with [I > 2σ(I)], 219 parameters, 0 restraints, R indices (all data) R_1 = 0.0447, wR_2 = 0.1053, final R indices [I > 2σ(I)] R_1 = 0.0388, wR_2 = 0.1023, largest difference peak and hole 0.363 and –0.634 e $Å^{-3}$, Goof = 1.076.

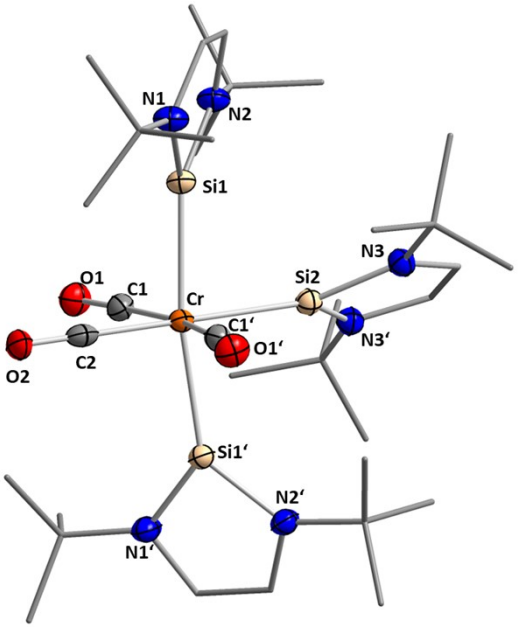

Figure S44. Molecular structure of $[Cr(CO)_3(tBu_2NHSi)_3]$ (**1**) in the solid state (ellipsoids set at the 50 % probability level). All hydrogen atoms are omitted for clarity. Selected bond lengths [Å] and angles [°]: Cr–Si1 2.328(1), Cr–Si2 2.365(1), Cr–C1 1.866(2), Cr–C2 1.838(3), C1–O1 1.160(3), C2–O2 1.160(4), Si1–Cr–Si2 85.300(17), Si1–Cr–Si1' 170.60(3), C1–Mo–C2 83.15(6), C1–Mo–C1' 166.30(13).

Crystal structure of [Mo(CO)$_3$(*t*Bu$_2$NHSi)$_3$] (2)

$C_{33}H_{60}Si_3N_6O_3Mo$, M_r = 769.08 g/mol, T = 99.99(10) K, λ = 1.54184 Å, colorless block, 0.02 × 0.12 × 0.13 mm^3, monoclinic, space group *C*2/c, a = 17.2683(2) Å, b = 11.16850(10) Å, c = 21.0161(2) Å, α = 90 °, β = 98.9250(10) °, γ = 90 °, V = 4004.11(7) Å^3, Z = 4, ρ_{calcd} = 1.276 Mg/m^3, μ = 3.843 mm^{-1}, F(000) = 1632, 20869 reflections, –21 ≤ h ≤ 21, –13 ≤ k ≤ 13, –19 ≤ l ≤ 25, 4.259 ° < θ < 75.107 °, completeness 99.5 %, 4007 independent reflections, 3867 reflections observed with [I > 2σ(I)], 356 parameters, 626 restraints, R indices (all data) R_1 = 0.0537, *w*R_2 = 0.1239, final R indices [I > 2σ(I)] R_1 = 0.0522, *w*R_2 = 0.1234, largest difference peak and hole 0.769 and –0.824 e Å^{-3}, Goof = 1.237.

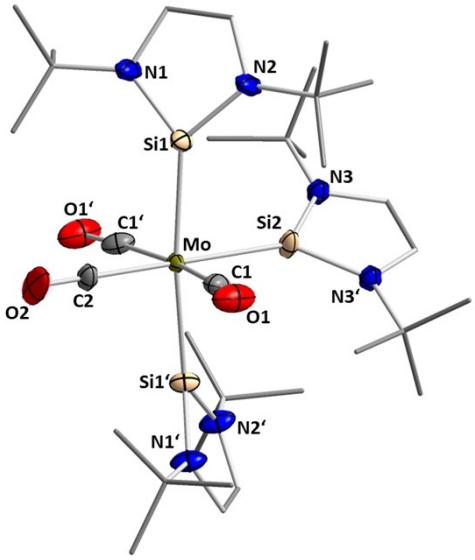

Figure S45. Molecular structure of [Mo(CO)$_3$(*t*Bu$_2$NHSi)$_3$] (**2**) in the solid state (ellipsoids set at the 50 % probability level). All hydrogen atoms are omitted for clarity. The structure of **2** shows disorder at both NHSi substituents, and the data corresponds to the part with (*trans*) 71 % and (*cis*) 67 % occupancy. Selected bond lengths [Å] and angles [°]: Mo–Si1 2.471(2), Mo–Si2 2.519(2), Mo–C1 2.027(5), Mo–C2 1.971(6), C1–O1 1.153(6), C2–O2 1.150(8), Si1–Mo–Si2 86.35(6), Si1–Mo–Si1' 172.69(12), C1–Mo–C2 84.74(16), C1–Mo–C1' 169.5(3).

Crystal structure of [Mo(Mes$_2$NHSi)$_3$(CO)$_3$] (3)

$C_{66}H_{75}Si_3N_6O_3Mo$, M_r = 1180.53 g/mol, T = 99.99(10) K, λ = 1.54184 Å, colorless block, 0.07 × 0.12 × 0.17 mm^3, triclinic, space group $P\bar{1}$, a = 12.07950(10) Å, b = 12.30430(10) Å, c = 22.1867(2) Å, α = 73.9570(10) °, β = 88.0480(10) °, γ = 77.9220(10) °, V = 3098.03(5) Å^3, Z = 2, ρ_{calcd} = 1.266 Mg/m^3, μ = 2.675 mm^{-1}, F(000) = 1242, 64475 reflections, –14 ≤ h ≤ 15, –15 ≤ k ≤ 14, –27 ≤ l ≤ 27, 3.743 ° < θ < 75.467 °, completeness 98.9 %, 12526 independent reflections, 11933 reflections observed with [I > 2σ(I)], 730 parameters, 0 restraints, R indices (all data) R_1 = 0.0259, wR_2 = 0.0649, final R indices [I > 2σ(I)] R_1 = 0.0247, wR_2 = 0.0643, largest difference peak and hole 0.424 and –0.611 e Å^{-3}, Goof = 1.053.

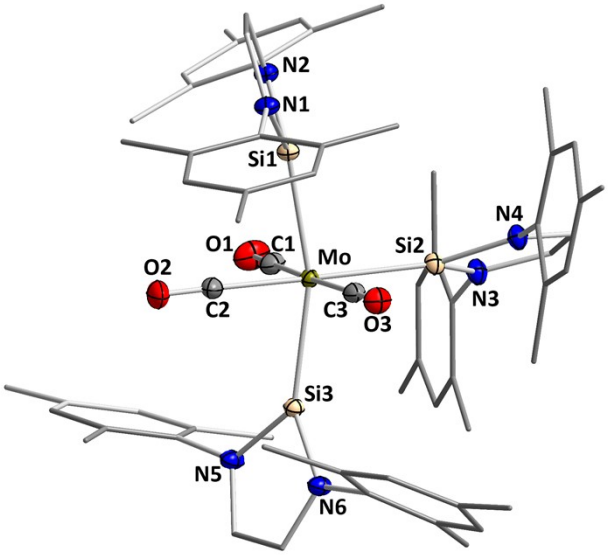

Figure S46. Molecular structure of [Mo(Mes$_2$NHSi)$_3$(CO)$_3$] (**3**) in the solid state (ellipsoids set at the 50 % probability level). All hydrogen atoms and co-crystalized solvent molecules (benzene) are omitted for clarity. Selected bond lengths [Å] and angles [°]: Mo–Si1 2.407(1), Mo–Si2 2.472(1), Mo–Si3 2.410(1), Mo–C1 2.041(2), Mo–C2 1.994(2), Mo–C3 2.038(2), C1–O1 1.145(2), C2–O2 1.155(2), C3–O3 1.144(2), Si1–Mo–Si2 96.804(13), Si1–Mo–Si3 163.132(14), Si2–Mo–Si3 99.974(13), C1–Mo–C2 96.47(6), C1–Mo–C3 176.14(6), C2–Mo–C3 87.39(6).

Crystal structure of $[Cr(CO)_3(Mes_2NHSi)_2(NCMe)]$ (4)

$C_{45}H_{51}Si_2N_5O_3Cr$, M_r = 818.09 g/mol, T = 100(2) K, λ = 1.54184 Å, yellow block, 0.11 × 0.34 × 0.53 mm^3, monoclinic, space group *C*c, a = 19.8409(3) Å, b = 13.67960(10) Å, c = 16.6891(2) Å, α = 90 °, β = 106.2790(10) °, γ = 90 °, V = 4348.08(9) $Å^3$, Z = 4, ρ_{calcd} = 1.250 Mg/m^3, μ = 3.045 mm^{-1}, F(000) = 1728, 22924 reflections, –24 ≤ h ≤ 24, –17 ≤ k ≤ 16, –20 ≤ l ≤ 19, 3.979 ° < θ < 75.265 °, completeness 99.7 %, 7101 independent reflections, 6810 reflections observed with [I > 2σ(I)], 519 parameters, 2 restraints, R indices (all data) R_1 = 0.0323, wR_2 = 0.0950, final R indices [I > 2σ(I)] R_1 = 0.0313, wR_2 = 0.0944, largest difference peak and hole 0.325 and –0.364 e $Å^{-3}$, Goof = 1.123.

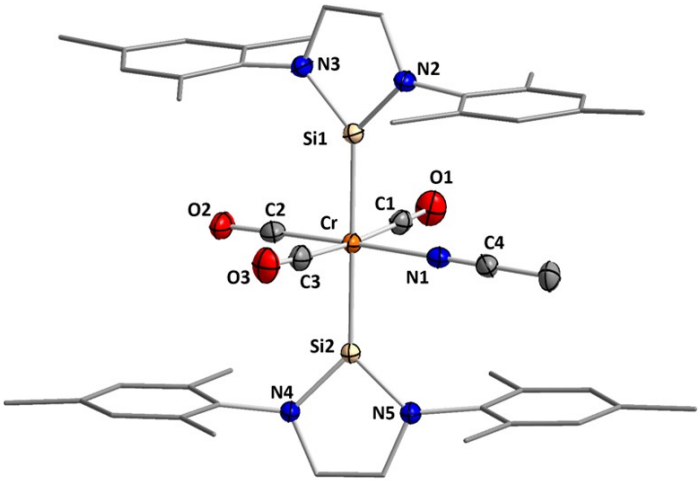

Figure S47. Molecular structure of $[Cr(CO)_3(Mes_2NHSi)_2(MeCN)]$ (**4**) in the solid state (ellipsoids set at the 50 % probability level). All hydrogen atoms are omitted for clarity. Selected bond lengths [Å] and angles [°] for **1**: Cr–Si1 2.256(1), Cr–Si2 2.271(1), Cr–C1 1.880(3), Cr–C2 1.880(4), Cr–C3 1.885(4), Cr–N1 2.045(3), N1–C4 1.131(4), C1–O1 1.159(4), C2–O2 1.164(4), C3–O3 1.153(5), C1–Cr–C3 175.99(12), C2–Cr–N1 178.54(15), Si1–Cr–Si2 179.16(5).

Crystal structure of $[Cr(CO)_3(Mes_2NHSi)_2(DMAP)]$ (7)

$C_{50}H_{58}Si_2N_6O_3Cr$, M_r = 899.20 g/mol, T = 100(2) K, λ = 1.54184 Å, orange block, 0.06 × 0.12 × 0.25 mm^3, monoclinic, space group $P2_1/n$, a = 10.8368(2) Å, b = 21.0245(3) Å, c = 20.9722(5) Å, α = 90 °, β = 91.746(2) °, γ = 90 °, V = 4776.05(16) $Å^3$, Z = 4, ρ_{calcd} = 1.251 Mg/m^3, μ = 2.824 mm^{-1}, F(000) = 1904, 45990 reflections, –12 ≤ h ≤ 13, –22 ≤ k ≤ 26, –26 ≤ l ≤ 25, 2.977 ° < θ < 75.160 °, completeness 98.6 %, 9437 independent reflections, 6580 reflections observed with [I > 2σ(I)], 573 parameters, 0 restraints, R indices (all data) R_1 = 0.0839, wR_2 = 0.1332, final R indices [I > 2σ(I)] R_1 = 0.0512, wR_2 = 0.1187, largest difference peak and hole 0.575 and –0.570 e $Å^{-3}$, Goof = 1.025.

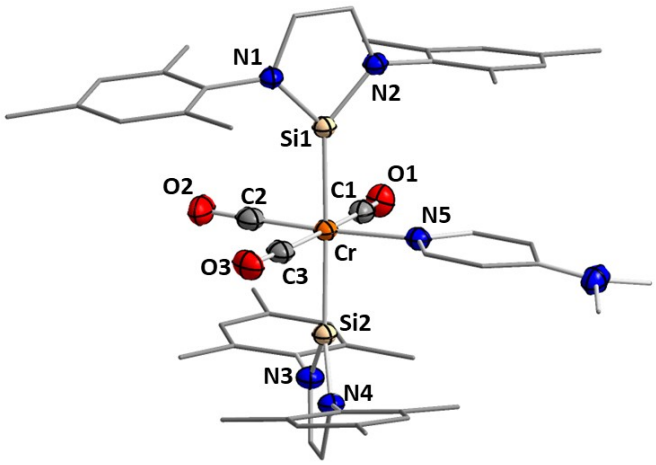

Figure S48. Molecular structure of $[Cr(CO)_3(Mes_2NHSi)_2(DMAP)]$ (**7**) in the solid state (ellipsoids set at the 50 % probability level). All hydrogen atoms are omitted for clarity. Selected bond lengths [Å] and angles [°]: Cr–Si1 2.279(1), Cr–Si2 2.280(1), Cr–C1 1.870(3), Cr–C2 1.822(3), Cr–C3 1.878(3), Cr–N5 2.193(2), C1–O1 1.168(3), C2–O2 1.182(4), C3–O3 1.161(3), Si1–Cr–Si2 177.62(4), Si1–Cr–C1 92.78(9), Si1–Cr–C2 89.06(9), Si1–Cr–C3 90.02(8), Si1–Cr–N5 88.44(6), Si2–Cr–N5 92.02(6), C1–Cr–C3 173.00(13), C2–Cr–N5 176.98(11).

Crystal structure of $[Cr(CO)_3(Mes_2NHSi)_2(CN\mathit{t}Bu)]$ (8)

$C_{48}H_{57}Si_2N_5O_3Cr$, M_r = 860.16 g/mol, T = 100(2) K, λ = 1.54184 Å, yellow block, 0.04 × 0.07 × 0.13 mm^3, monoclinic, space group *C*2/c, a = 16.5398(2) Å, b = 15.1355(2) Å, c = 18.5302(2) Å, α = 90 °, β = 91.4820(10) °, γ = 90 °, V = 4637.26(10) Å^3, Z = 4, ρ_{calcd} = 1.232 Mg/m^3, μ = 2.878 mm^{-1}, F(000) = 1824, 24084 reflections, –19 ≤ h ≤ 20, –18 ≤ k ≤ 17, –22 ≤ l ≤ 22, 3.960 ° < θ < 73.758 °, completeness 100 %, 4627 independent reflections, 3794 reflections observed with [I > 2σ(I)], 300 parameters, 9 restraints, R indices (all data) R_1 = 0.0569, wR_2 = 0.1229, final R indices [I > 2σ(I)] R_1 = 0.0459, wR_2 = 0.1161, largest difference peak and hole 0.553 and –0.437 e Å^{-3}, Goof = 1.026.

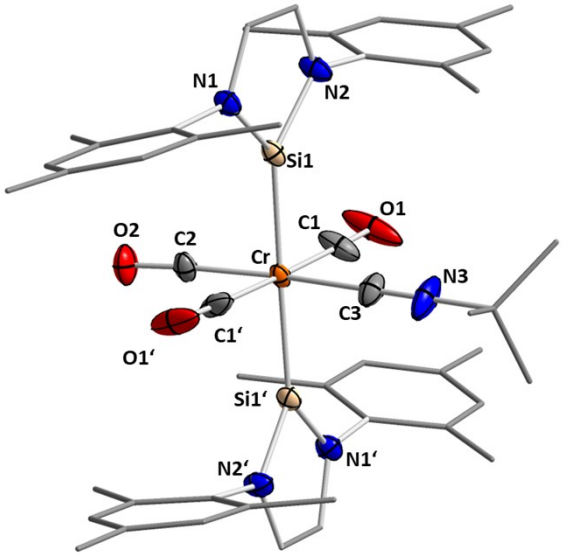

Figure S49. Molecular structure of $[Cr(CO)_3(Mes_2NHSi)_2(CN\mathit{t}Bu)]$ (**8**) in the solid state (ellipsoids set at the 30 % probability level). All hydrogen atoms are omitted for clarity. Selected bond lengths [Å] and angles [°]: Cr–Si1 2.257(1), Cr–C1 1.877(3), Cr–C2 1.846(4), Cr–C3 1.956(3), C1–O1 1.148(3), C2–O2 1.166(5), C3–N3 1.167(4), Si1–Cr–Si1' 178.75(4), Si1–Cr–C1 90.33(8), Si1–Cr–C2 90.4(3), Si1–Cr–C3 89.37(2), C1–Cr–C2 97.82(15), C1'–Cr–C2 79.39(15), C1–Cr–C1' 177.2(2), C2–Cr–C3 170.78(11).